REFERENCES

[1] Kaminsky, W. and Laban, A. Metallocene catalysis. **Applied Catalysis A: General** 222 (2001): 47-61.

[2] Quijada, R.; Retuert, J.; Guevara, J.L.; Rojas, R.; Valle, M.; Saavedra, P.; Palza, H. and Galland, G.B. Results Coming from Homogeneous and Supported Metallocene Catalysts in the Homo- and Copolymerization of Olefins. **Macromol. Symp.** 189 (2002): 111-125.

[3] Lee, K-S.; Oh, C-G.; Yim, J-H. and Ihm, S-K. Characterization of zirconocene catalysts supported on Al-MCM-41 for ethylene polymerization. **J. Mol. Catal. A: Chem.** 159 (2000): 301-308.

[4] Charoenchaidet, S.; Chavadej, S. and Gulari, E. Borane-functionalized silica supports In situ activated heterogeneous zirconocene catalysts for MAO-free ethylene polymerization. **J. Mol. Catal. A: Chem.** 185 (2002): 167-177.

[5] Rahiala, H.; Beurroies, I.; Eklund, T.; Hakala, K.; Gougeon, R.; Trens, P. and Rosenholm, J.B. Preparation and Characterization of MCM-41 Supported Metallocene Catalysts for Olefin Polymerization. **J. Catal.** 188 (1999): 14-23.

[6] Galland, G.B.; Seferin, M.; Mauler, R.S. and dos Santos, J.H.Z. Linear low-density polyethylene synthesis promoted by homogeneous and supported catalysts. **Polym. Int.** 48 (1999): 660-664.

[7] Galland, G.B.; Seferin, M.; Guimarães, R.; Rohrmann, J.A.; Stedile, F.C. and dos Santos, J.H.Z. Evaluation of silica-supported zirconocene in ethylene/1-hexene copolymerization. **J. Mol. Catal. A: Chem.** 189 (2002): 233-240.

[8] Dong X.; Wang L.; Wang W.; Yu H.; Wang J.; Chen T. and Zhao Z. Preparation of nano-polyethylene fibers and floccules using MCM-41-supported metallocene catalytic system under atmospheric pressure. **Euro. Polym. J.** 41 (2005): 797-803.

[9] Jongsomjit, B.; Kaewkrajang, P.; Wanke, S.E. and Praserthdam, P. A comparative study of ethylene/α-olefin copolymerization with silane-modified silica-supported MAO using zirconocene catalysts. **Catal. Lett.** 94 (2004): 205-208.

[10] Jongsomjit, B.; Praserthdam, P. and Kaewkrajang, P. A comparative study on supporting effect during copolymerization of ethylene/1-olefins with silica-supported zirconocene/MAO catalyst. **Mater. Chem. Phys.** 86 (2004): 243-246.

[11] Jongsomjit, B.; Kaewkrajang, P.; Shiono, T. and Praserthdam, P. Supporting Effect of Silica-Supported Methylaluminoxane (MAO) with Zirconocene Catalyst on Ethylene/1-Olefin Copolymerization Behaviors for Linear Low-Density Polyethylene (LLDPE) Production. **Ind. Eng. Chem. Res.** 43 (2004): 7959-7963.

[12] Britcher, L.; Rahiala, H.; Hakala, K.; Mikkola, P. and Rosenholm, J.B. Preparation, Characterization, and Activity of Silica Supported Metallocene Catalysts. **Chem. Mater.** 16 (2004): 5713-5720.

[13] Jongsomjit, B.; Ngamposri, S. and Preserthdam, P. Role of titania in TiO_2-SiO_2 mixed oxides-supported metallocene catalyst during ethylene/1-octene copolymerization. **Catal. Lett.** 100 (2005): 139-146.

[14] Jongsomjit, B.; Ngamposri, S. and Preserthdam, P. Catalytic Activity During Copolymerization of Ethylene and 1-Hexene via Mixed TiO_2/SiO_2-Supported MAO with *rac*-Et$[Ind]_2ZrCl_2$ Metallocene Catalyst. **Molecules.** 10 (2005): 603- 609.

[15] Ko, Y.S. and Woo, S.I. Copolymerization of Ethylene and α-Olefin Using $Et(Ind)_2ZrCl_2$ Entrapped inside the Regular and Small Pores of MCM-41. **Macromol. Chem. Phys.** 202 (2001): 739-744.

[16] Beck, J.S.; Vartuli, J.C.; Roth, W.J.; Leonowicz, M.E.; Kresge, C.T.; Schmitt, K.D.; Chu, C.T-W.; Olson, D.H.; Sheppard, E.W.; McCullen, S.B.; Higgins, J.B. and Schlenker, J.L. A New Family of Mesoporous Molecular Sieves Prepared with Liquid Crystal Templates. **J. Am. Chem. Soc.** 114 (1992): 10834-10843.

[17] Sayari, A.; Danumaha, C. and Moudrakovski, I.L. Boron-Modified MCM-41 Mesoporous Molecular Sieves. **Chem. Mater.** 7 (1995): 813-815.

[18] On, D.T.; Joshi, P.N. and Kaliaguine, S. Synthesis, Stability and State of Boron in Boron-Substituted MCM-41 Mesoporous Molecular Sieves. **J. Phys. Chem.** 100 (1996): 6743-6748.

[19] Scheirs, J. and Kaminsky, W. **Metallocene-based Polyolefins.** vol. 1, West Sussex, :Wiley, 2000.

[20] Naga, N. and Imanishi, Y. Recent developments in olefin polymerizations with transition metal catalysts. **Prog. Polym. Sci.** 26 (2001): 1147-1198.

[21] Gupta, V.K.; Satish, S. and Bhardwaj, I.S.J.M.S. Metallocene complexes of group-4 elements in the polymerization of monoolefins. **Rev. Macromol. Chem. Phys. C** 34(3) (1994): 439-514.

[22] Kaminsky, W. **Metalorganic Catalysts for Synthesis and Polymerization.** Springer, 1999.

[23] Brintzinger, H.H.; Fischer, D.; Mulhaupt, R.; Rieger, B. and Waymouth, R.M. Stereospecific Olefin Polymerization with Chiral Metallocene Catalysts. **Angew. Chem. Int. Ed. Engl.** 34 (1995): 1143-1170.

[24] Britovsek, G.J.P.; Gibson, V.C. and Wass, D.F. The Search for New-Generation Olefin Polymerization Catalysts: Life Beyond Metallocenes. **Angew. Chem. Int. Ed. Engl.** 38 (1999): 429-447.

[25] Hlatky, G.G. Metallocene Catalysts for Olefin Polymerization Annual Review For 1996. **Coordination Chem. Rev.** 181 (1999) 243-296.

[26] Bajgur, C.S. and Sivaram, S. The Evaluation Of New Generation "Single-Site" Ziegler-Natta Polymerization Catalysts. **Curr.Sci.** 78 (11) (2000): 1325-1335.

[27] Alt, H.G. and Koppl, A. Effect of the Nature of Metallocene Complexes of Group IV Metals on Their Performance in Catalytic Ethylene and Propylene Polymerization. **Chem. Rev.** 100 (2000): 1205-1221.

[28] Rappe, A.K.; Skiff, W.M. and Casewit, C.J. Modeling Metal-Catalyzed Olefin Polymerization. **Chem. Rev.** 100 (2000): 1435-1456.

[29] Xie, T.; Mcauley, K.B.; Hsu, J.C.C. and Bacon, D.W. Gas Phase Ethylene Polymerization: Production Processes, Polymer Properties and Reactor Modeling. **Ind. Eng. Chem. Res.** 33 (1994): 449-479.

[30] Alt, H. The Heterogenization of Homogeneous Metallocene Catalysts for Olefin Polymerization. **J. Chem. Soc.**; Dalton Transactions (1999): 1703-1709.

[31] Coates, G.W. Precise Control of Polyolefin Stereo Chemistry Using Single-Site Metal Catalysts. **Chem. Rev.** 100 (2000): 1223-1252.

[32] Castonguay, L. A. and Rappe, A. K. **J. Am. Chem. Soc.** 114 (1992): 5832- 5842.

[33] Huang, J. and Rempel, G. L Ziegler-Natta Catalysts for Olefin Polymerization: Mechanistic Insights from Metallocene Systems. **Prog. Polym. Sci.** 20 (1995): 459-526.

[34] Pédeutour, J.N.; Radhakrishnan, K.; Cramail, H. and Deffieux, A. Use of "TMA-depleted" MAO for the activation of zirconocene in olefin polymerization. **J. Mol. Catal. A: Chem.** 185 (2002): 119-125.

[35] Chen, E.Y.X. and Marks, T.J. Cocatalysts for Metal-Catalyzed Olefin Polymerization: Activators, Activation Processes and Structure-Activity Relationships. **Chem. Rev.** 100 (2000): 1391-1434.

[36] Pédeutour, J.N.; Radhakrishnan, K.; Cramail, H. and Deffieux, A. Influence of X ligand nature in the activation process of *rac*Et(Ind)$_2$ZrX$_2$ by methylaluminoxane. **J. Mol. Catal. A: Chem.** 176 (2001): 87-94.

[37] Cam, D. and Giannini, U. **Makromol. Chem.** 193 (1992): 1049-1055.

[38] Soga, K.; Kim, H. J. and Shiono, T. Polymerization of Ethylene with Homogeneous Metallocene Catalysts Activated By Common Trialkylaluminums and Si(CH$_3$)$_3$OH. **Makromol. Chem. Rapid Commun.** 14 (1993): 765-770.

[39] Katayama, H.; Shiraishi, H.; Hino, T.; Ogane, T. and Imai, A. The Effect of Aluminum Compounds in the Copolymerization of Ethylene α-Olefins. **Macromol. Symp.** 97 (1995): 109-118.

[40] Przybyla, C.; Tesche, B. and Fink, G. Ethylene hexane copolymerization with the heterogeneous catalyst system SiO$_2$/MAO/rac-Me$_2$Si[2-Me-4-Ph-Ind]2ZrCl2: The filter effect. **Macromol. Rapid Commun**. 20 (1999): 328-332.

[41] Harkki, O.; Lehmus, P.; Leino, R.; Luttikhedde, H. J. G.; Nasman, J. H. and Seppala, J. V. Copolymerzation of ethylene with 1-hexene or 1-hexadecene over siloxy-substituted. **Macromol. Chem. Phys.** 200 (1999): 1561-1565.

[42] Cheruvu, S. **US Pat 5608019** (1997).

[43] Albano, C.; Sanchez, G. and Ismayel, A. Influence of a copolymer on the mechanical properties of a blend of PP and recycled and non-recycled HDPE. **Polym. Bull.** 41 (1998): 91-98.

[44] Shan, C. L. P.; Soares, J. B. P. and Penlidis, A. Ethylene/1-octene copolymerization studies with in situ supported metallocene catalysts: Effect of polymerization parameters on the catalyst activity and polymer microstructure. **J. Polym. Sci.: Part A: Polym Chem.** 40 (2002): 4426-4451.

[45] Pietikainen, P. and Seppala, J.V. Low Molecular Weight Ethylene/Propylene Copolymers. Effect of Process Parameters on Copolymerization with Homogeneous Cp_2ZrCl_2 Catalyst. **Macromolecules** 27 (1994): 1325-1328.

[46] Soga, K. and Kaminaka, M. **Macromol. Chem. Rapid Commun.** 13 (1992): 221-224.

[47] Nowlin, T. E.; Kissin, Y. V. and Wagner, K. P. High activity Ziegler-Natta catalyst for the preparation of ethylene copolymers. **J. Polym. Sci.: Part A: Polym.Chem.** 26 (1988): 755-764.

[48] Quijada, R.; Galland, G. B. and Mauler, R. S. **Macromol. Chem. Phys.** 197 (1996): 3091-3098.

[49] Soga, K.; Uozumi, T.; Arai, T. and Nakamura, S. Heterogeneity of Active Species in Metallocene Catalysts. **Macromol. Rapid Commun.** 16 (1995): 379-385.

[50] de Fatima V. Marques, M.; Conte, A. F.; de Resende, C. and Chaves, E. G. Copolymerization of ethylene and 1-octene by homogeneous and different supported metallocenic catalysts. **J. App. Polym. Sci.** 82 (2001): 724-730.

[51] Kim, J. D. and Soares, J. B. P. Copolymerization of ethylene and 1-hexene with supported metallocene catalysts: Effect of support treatment. **Macromol. Rapid Commun.** 20 (1999): 347-350.

[52] Chu, K. J.; Shan, C. L. P.; Soares, J. B. P. and Penlidis, A. Copolymerization of ethylene and 1-hexene with in-situ supported $Et[Ind]_2ZrCl_2$. **Macromol. Chem. Phys.** 200 (1999): 2372-2376.

[53] Chu, K. J.; Soares, J. B. P. and Penlidis, A. Variation of molecular weight distribution (MWD) and short chain branching distribution (SCBD) of ethylene/1-hexene copolymers produced with different in-situ supported metallocene catalysts. **Macromol. Chem. Phys.** 201 (2000): 340-348.

[54] Shan, C. L. P.; Chu, K. J.; Soares, J.B.P. and Penlidis, A. Using alkylaluminum activators to tailor short chain branching distributions of ethylene/1-hexene copolymers produced with in-situ supported metallocene catalysts. **Macromol. Chem. Phys.** 201 (2000): 2195-2202.

[55] Chu, K.J.; Soares, J.B.P. and Penlidis, A. Polymerization mechanism for in situ supported metallocene catalysts. **J. Polym. Sci.: Part A: Polym. Chemetry.** 38 (2000): 462-468.

[56] Chu, K.J.; Shan, C.L.P.; Soares, J.B.P. and Penlidis, A. **Macromol. Chem. Phys.** 198 (1997): 304-348.

[57] Zhao, X.S.; Lu, G.Q.(Max) and Millar, G.J. Advances in Mesoporous Molecular Sieve MCM-41. **Ind. Eng. Chem. Res.** 35 (1996): 2075-2090.

[58] Corma, A. From microporous to mesoporous molecular sieve materials and their use in catalysis. **Chem. Rev.** 97 (1997): 2373-2419.

[59] Panpranot, J.; Pattamakomsan, K.; Goodwin J.G. and Praserthdam, P. A comparative study of Pd/SiO_2 and Pd/MCM-41 catalysts in liquid-phase hydrogenation. **Catal. Commun.** 5 (2004): 583-590.

[60] Li , J. and Coville, N.J. The effect of boron on the catalyst reducibility and activity of Co/TiO_2 Fischer-Tropsch catalysts. **App. Catal. A.** 181 (1999): 201-208.

[61] Randall, J.C. A review of high-resolution liquid ^{13}carbon nuclear magnetic resonance characterizations of ethylene-based polymer. **Macromol. Chem. Phys.** C29 (1989): 201.

[62] Jongsomjit, B.; Ngamposri, S. and Praserthdam, P. Application of Silica/Titania Mixed Oxide-Supported Zirconocene Catalysts for Synthesis of Linear Low-Density Polyethylene. **Ind. Eng. Chem. Res.** 44 (2005): 9059-9063.

[63] Hagimoto, H.; Shiono, T. and Ikeda, T. Supporting Effects of Methylaluminoxane on Living Polymerization of Propylene with a Chelating (Diamide)dimethyl titanium Complex. **Macromol. Chem. Phys.** 205 (2004): 19-26.

[64] Galland, G.B.; Quijada, P.; Mauler, R.S. and de Menezes, S.C. Determination of reactivity ratios for ethylene/α-olefin copolymerization catalysed by the $C_2H_4[Ind]_2ZrCl_2$/methylaluminoxane system. **Macromol. Rapid. Commun.** 17 (1996): 607-613.

[65] Chaichana, E.; Jongsomjit, B. and Prasethdam, P. Effect of nano-SiO_2 particle size on the formation of LLDPE/SiO_2 nanocomposite synthesized via the in situ polymerization with metallocene catalyst. **Chem. Eng. Sci.** 62 (2007): 899-905.

[66] Liu, S.; Yu, G. and Huang B. Polymerization of ethylene by zirconocene $B(C_6F_5)_3$ catalysts with aluminum compounds. **J. App. Polym. Sci.** 66 (1997): 1715-1720.

APPENDICES

APPENDIX A
(Nuclear Magnetic Resonance)

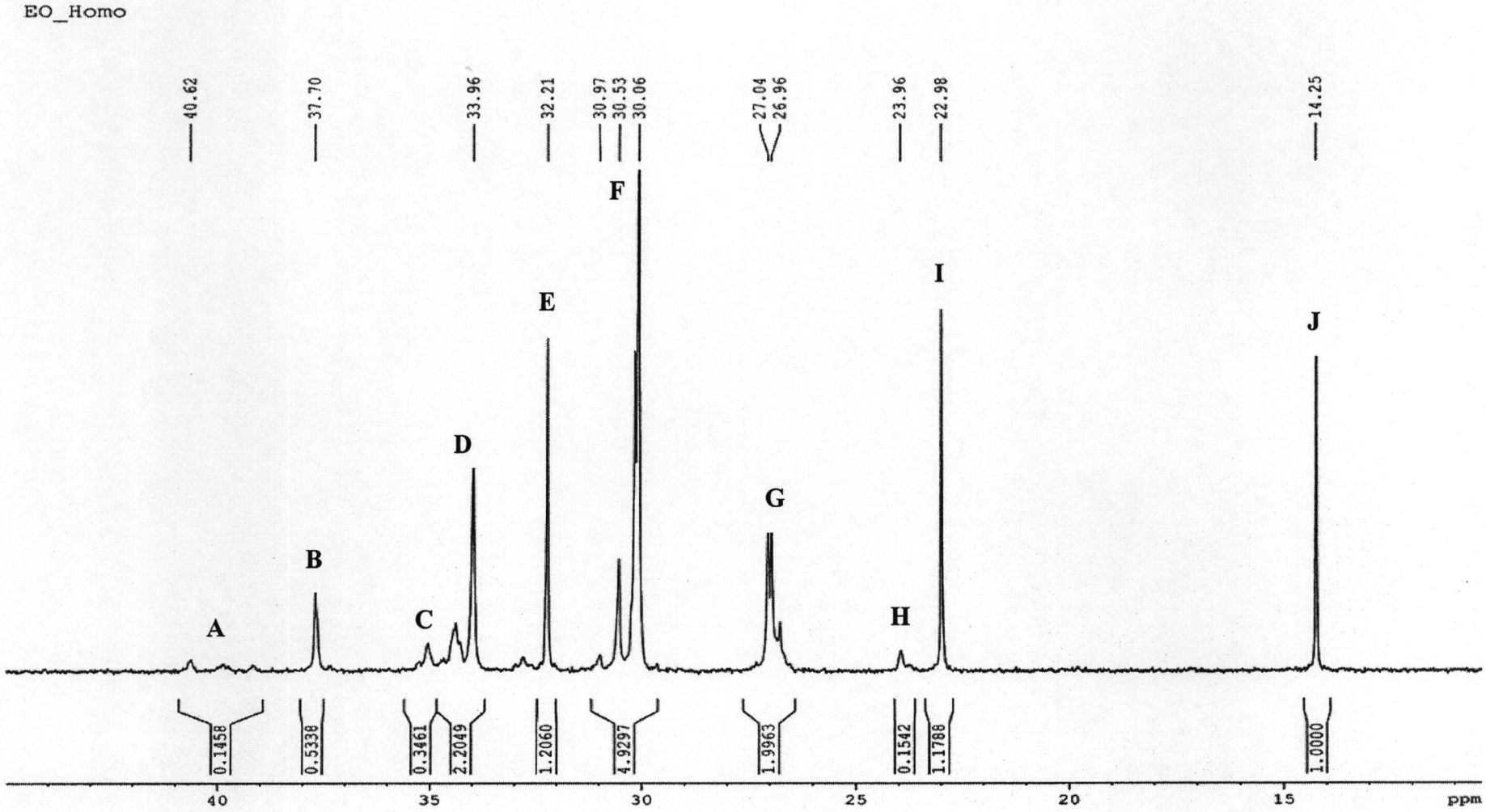

Figure A-1. ^{13}C-NMR spectrum of ethylene/1-octene copolymer produce with homogeneous

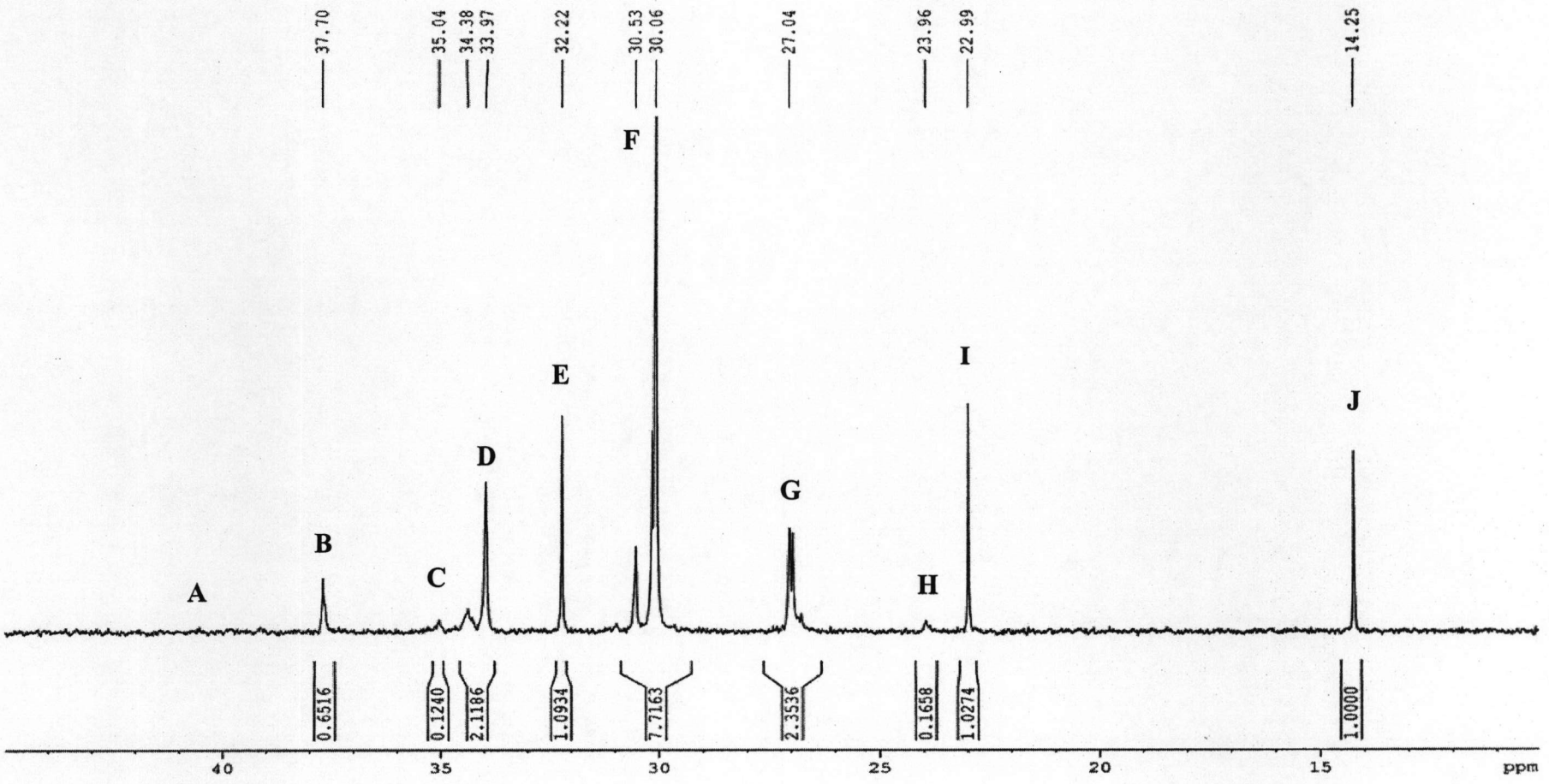

Figure A-2. [13] C-NMR spectrum of ethylene/1-octene copolymer produce with MCM-41 small pore

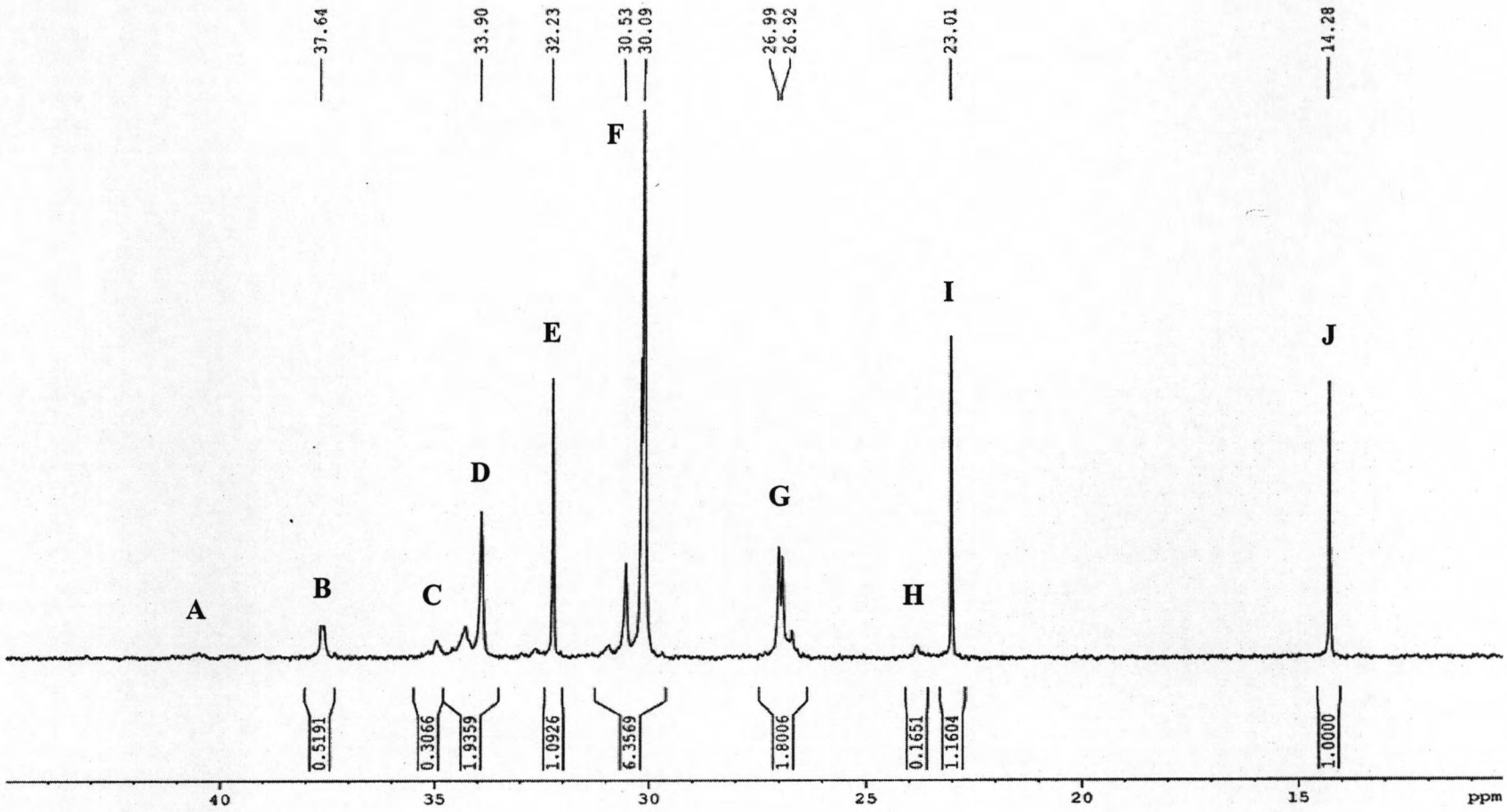

Figure A-3. [13] C-NMR spectrum of ethylene/1-octene copolymer produce with MCM-41 small pore via 1%wt of boron loading

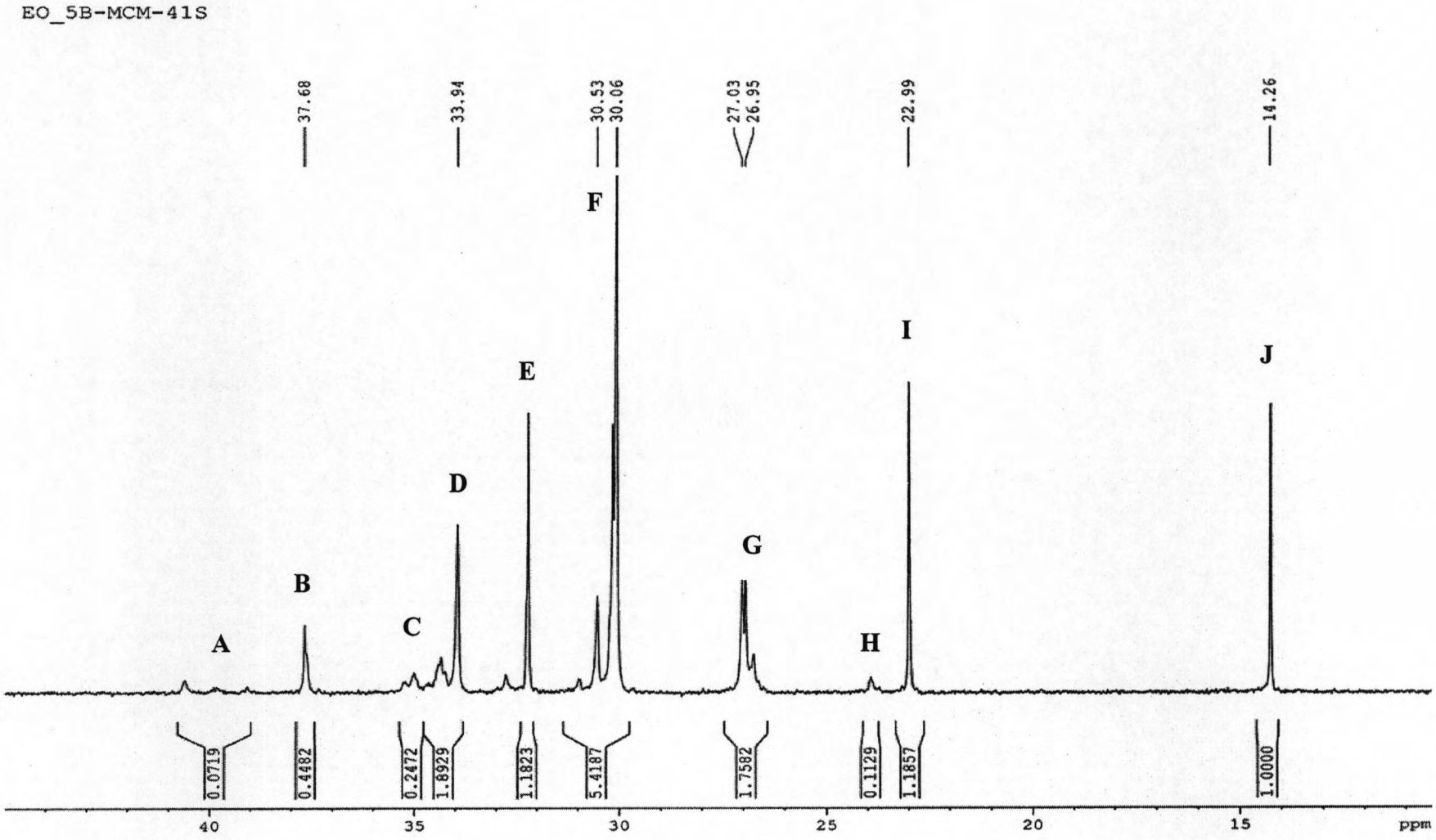

Figure A-4. [13] C-NMR spectrum of ethylene/1-octene copolymer produce with MCM-41 small pore via 5%wt of boron loading

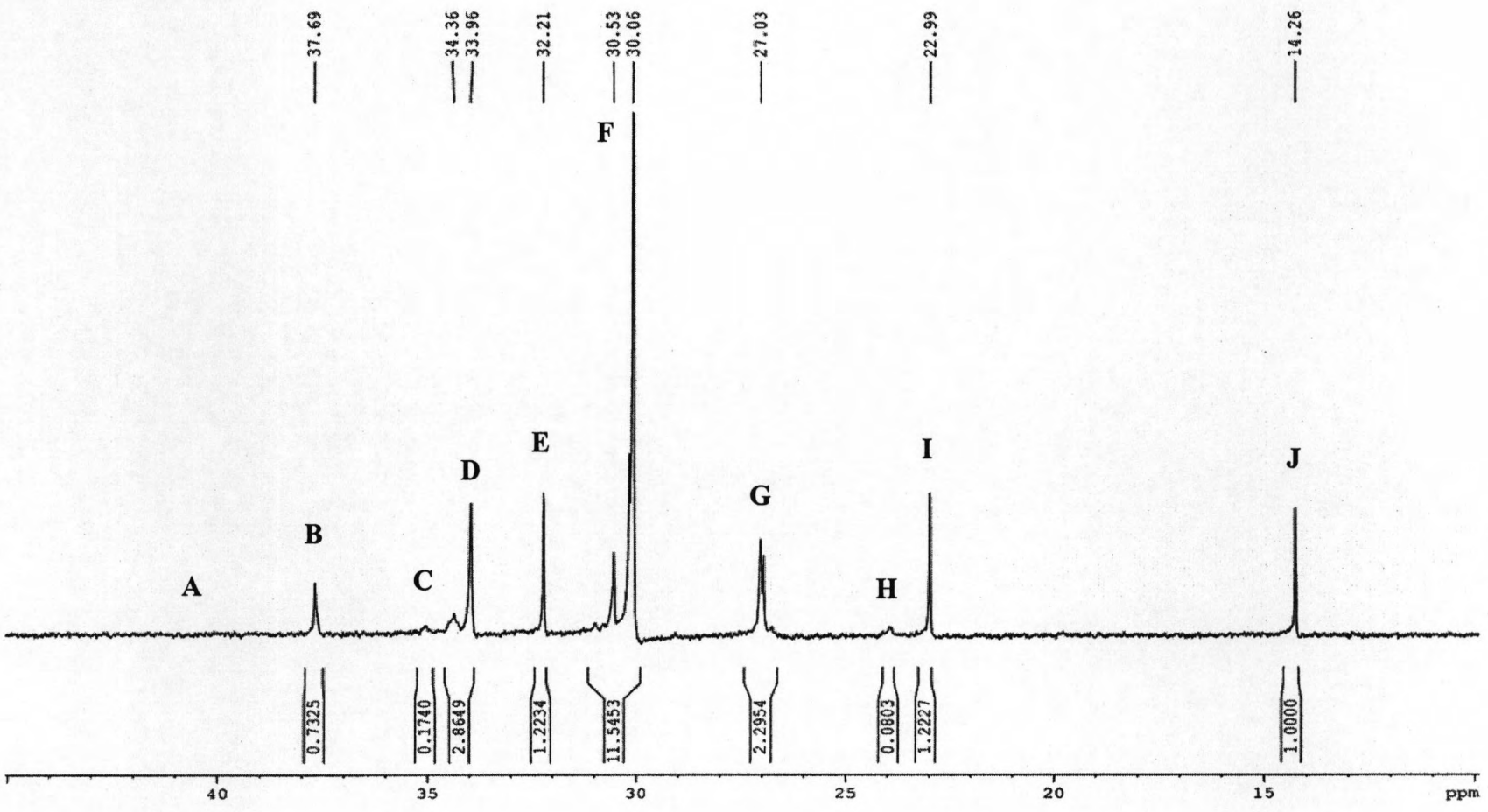

Figure A-5. ^{13}C-NMR spectrum of ethylene/1-octene copolymer produce with MCM-41 large pore

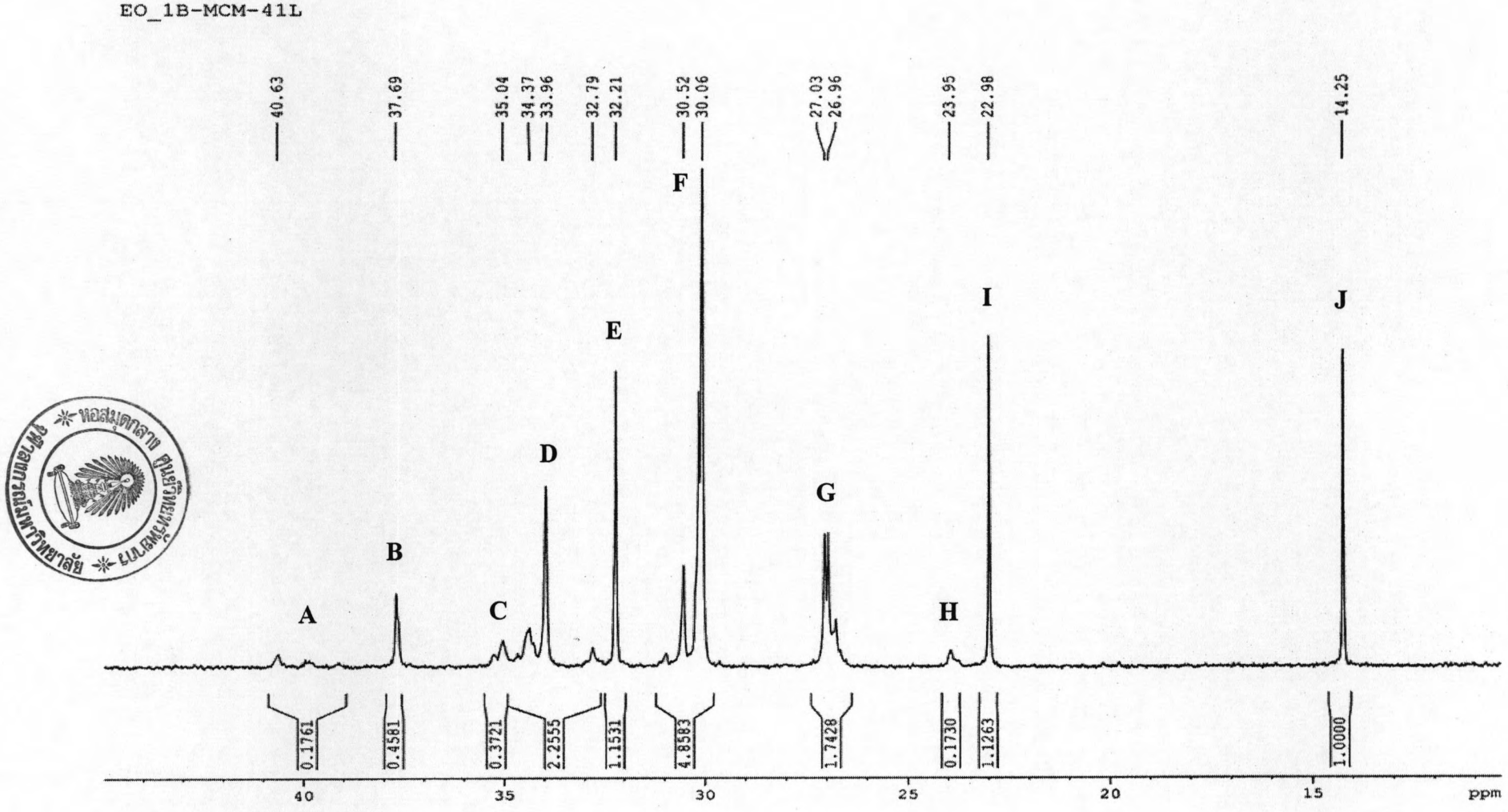

Figure A-6. ^{13}C-NMR spectrum of ethylene/1-octene copolymer produce with MCM-41 large pore via 1%wt of boron loading

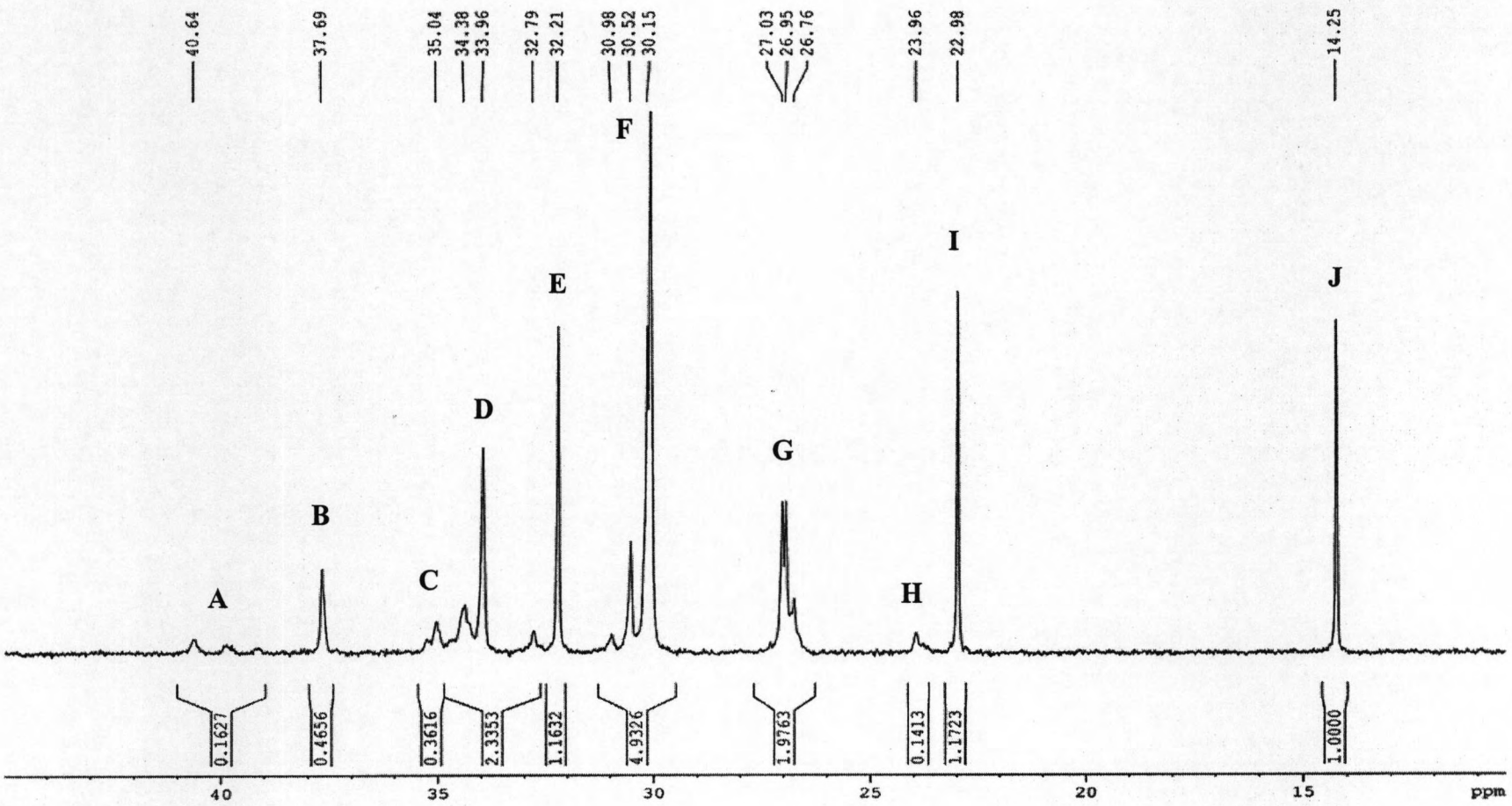

Figure A-7. ^{13}C-NMR spectrum of ethylene/1-octene copolymer produce with MCM-41 large pore via 5%wt of boron loading

APPENDIX B
(Differential Scanning Calorimeter)

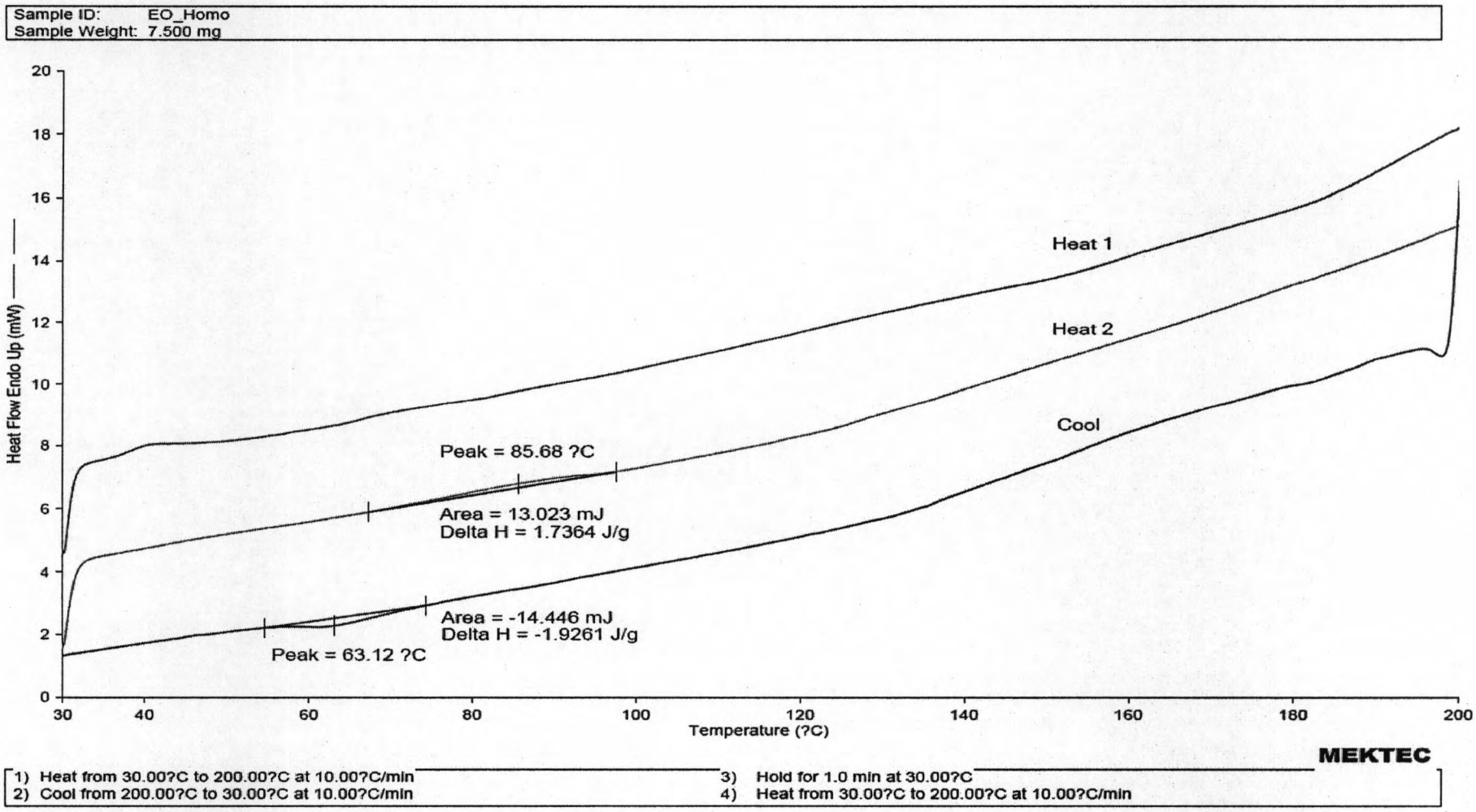

Figure B-1. DSC curve of ethylene/1-octene copolymer produce with homogeneous

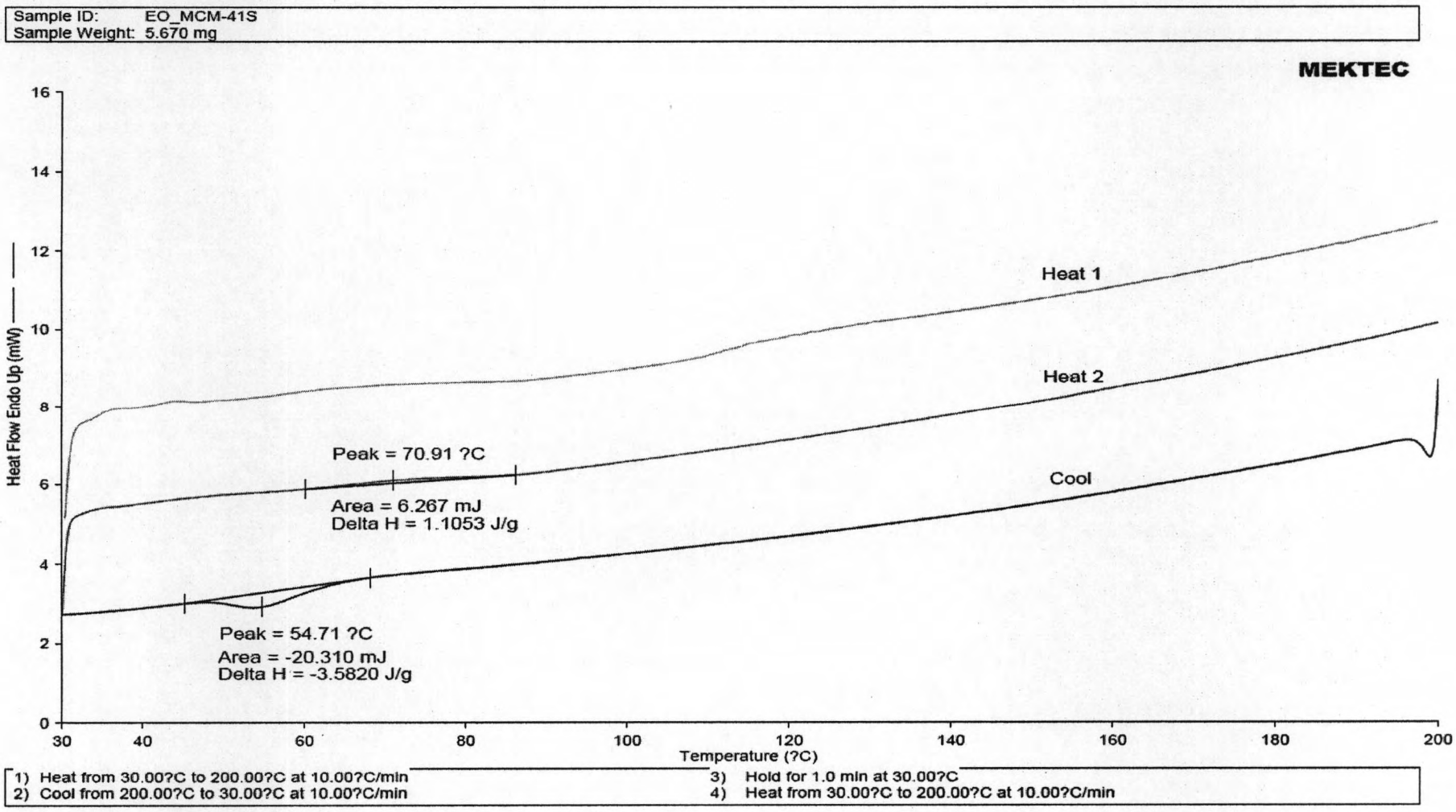

Figure B-2. DSC curve of ethylene/1-octene copolymer produce with MCM-41 small pore

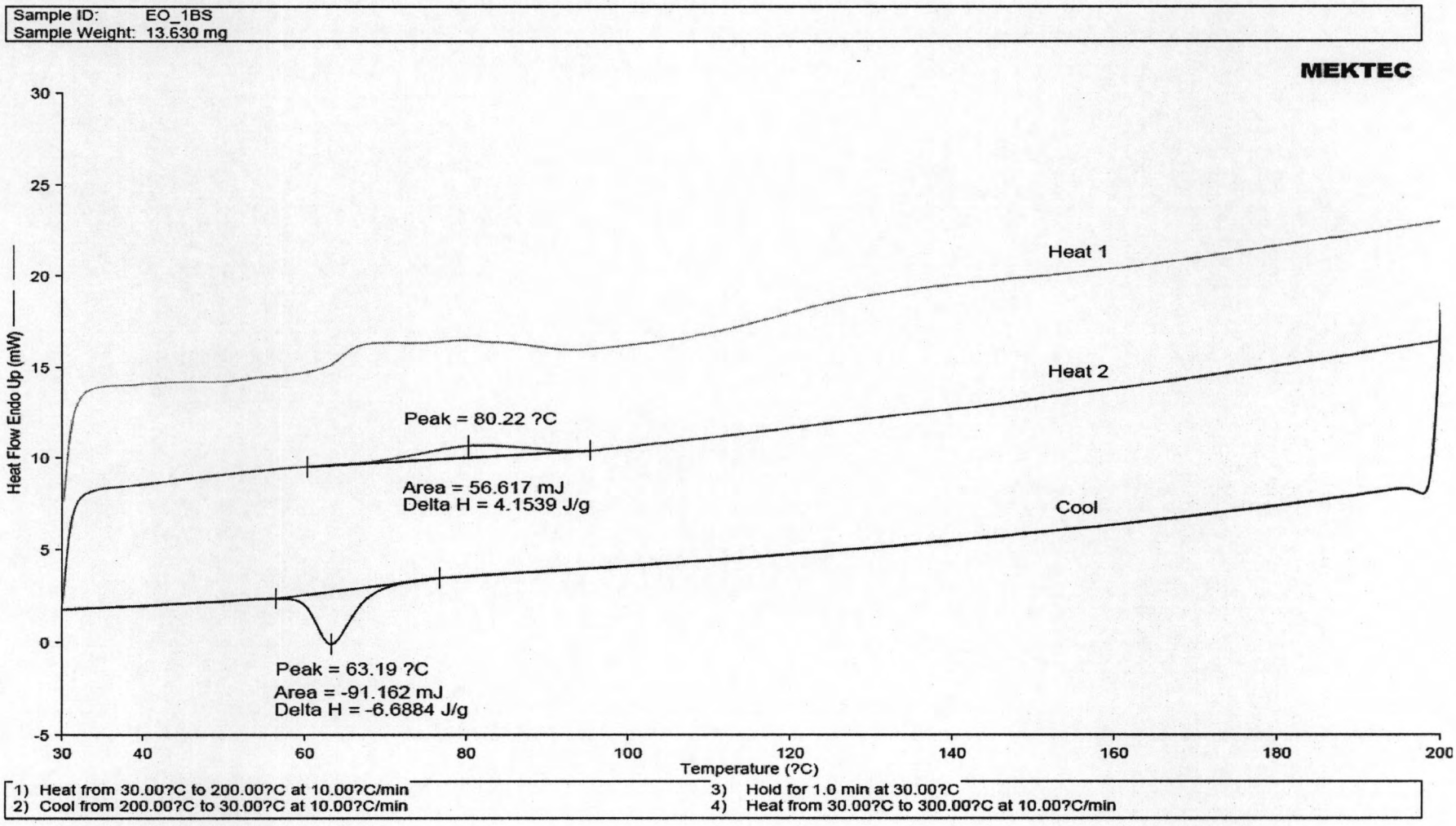

Figure B-3. DSC curve of ethylene/1-octene copolymer produce with MCM-41 small pore via 1%wt of boron loading

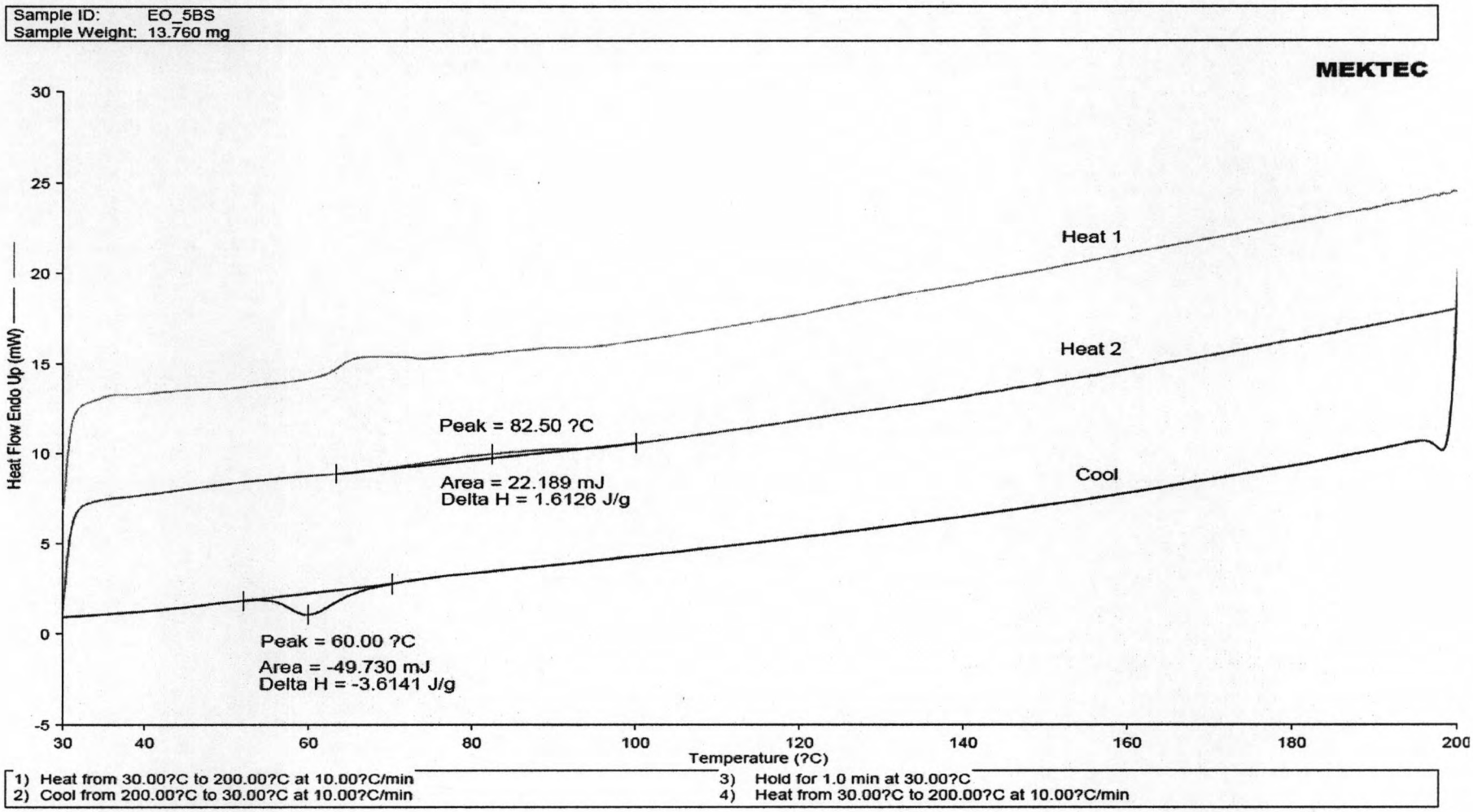

Figure B-4. DSC curve of ethylene/1-octene copolymer produce with MCM-41 small pore via 5%wt of boron loading

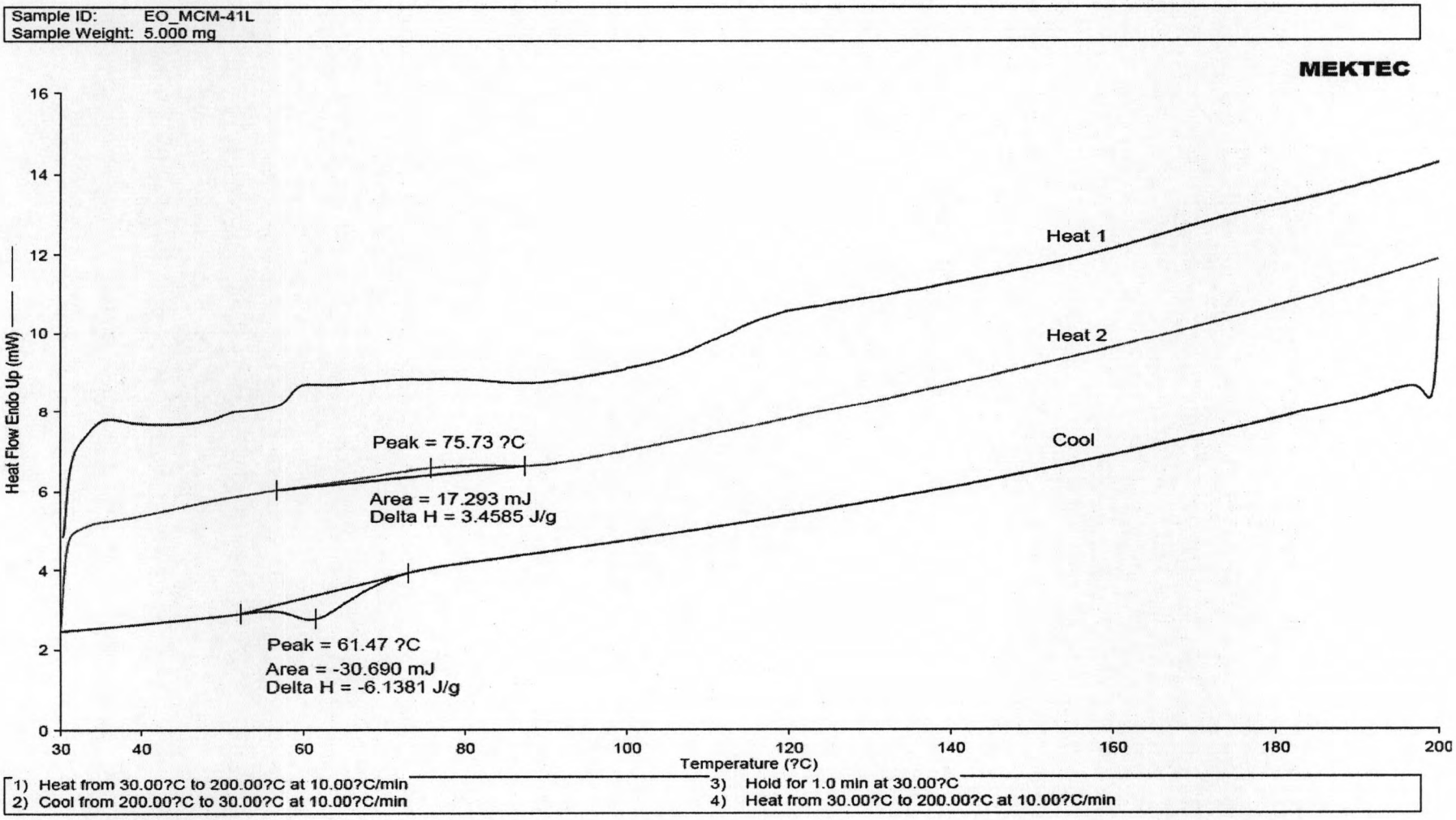

Figure B-5. DSC curve of ethylene/1-octene copolymer produce with MCM-41 large pore

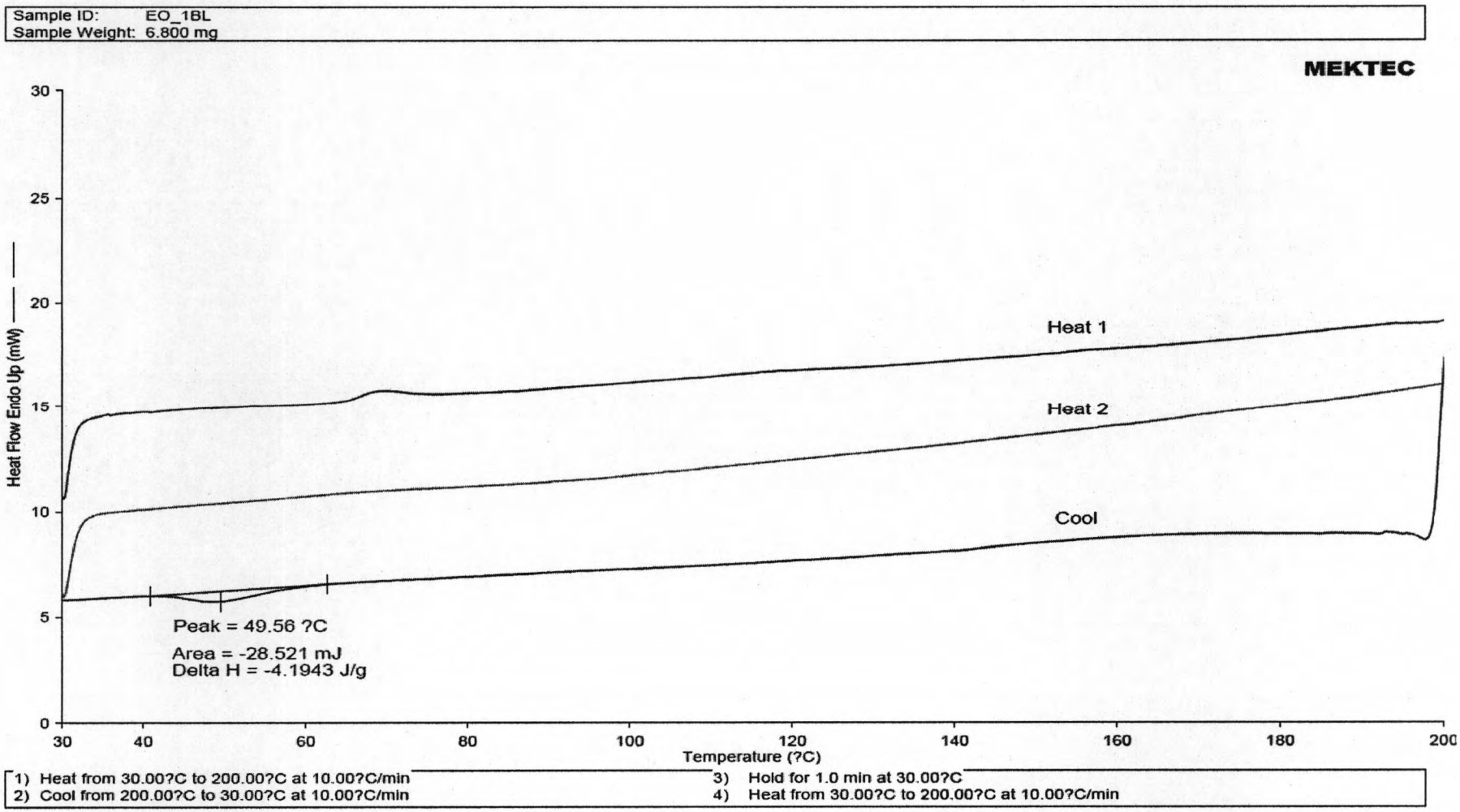

Figure B-6. DSC curve of ethylene/1-octene copolymer produce with MCM-41 large pore via 1%wt of boron loading

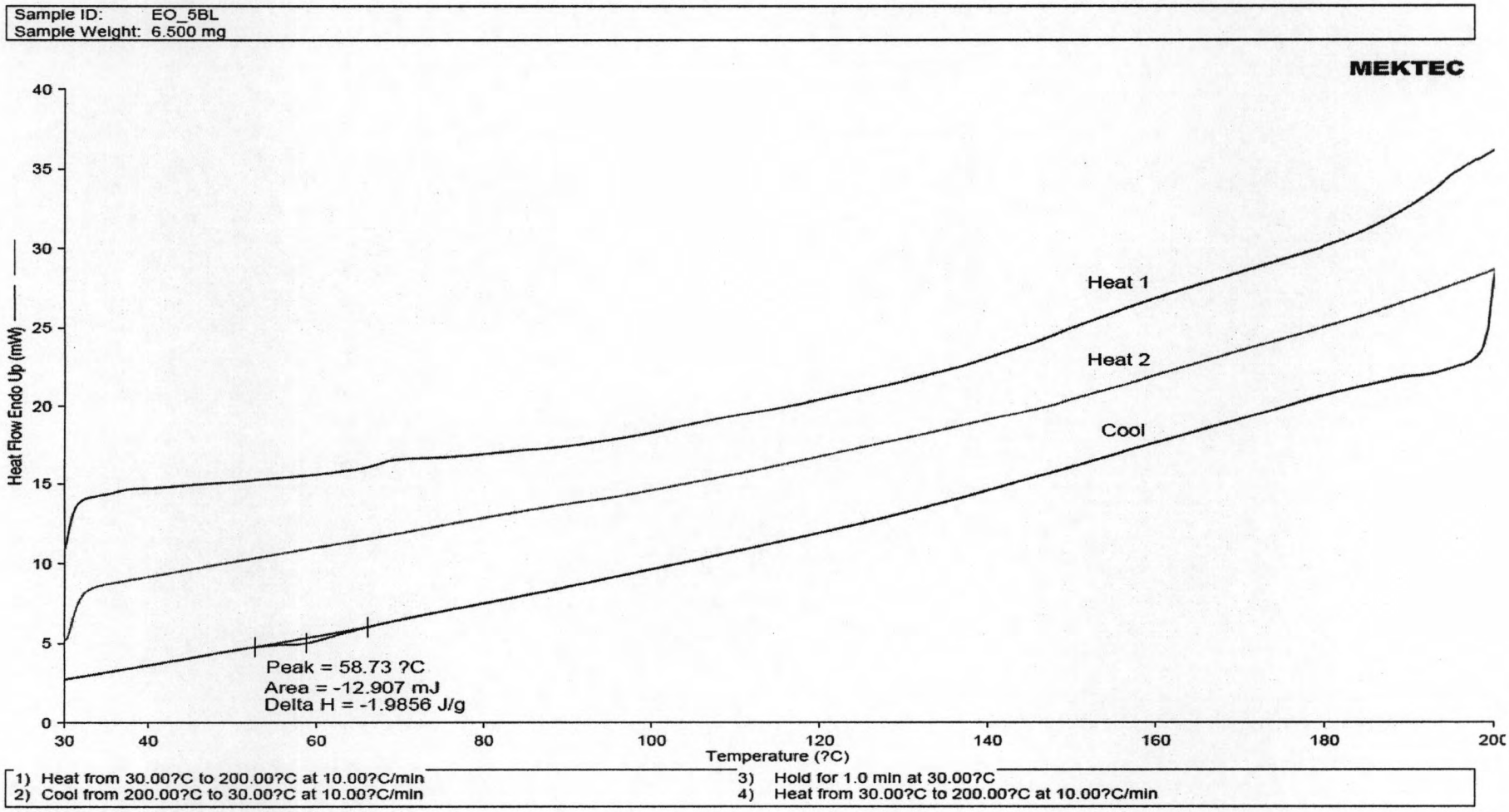

Figure B-7. DSC curve of ethylene/1-octene copolymer produce with MCM-41 large pore via 5%wt of boron loading

APPENDIX C
(Gel Permeation Chromatrography)

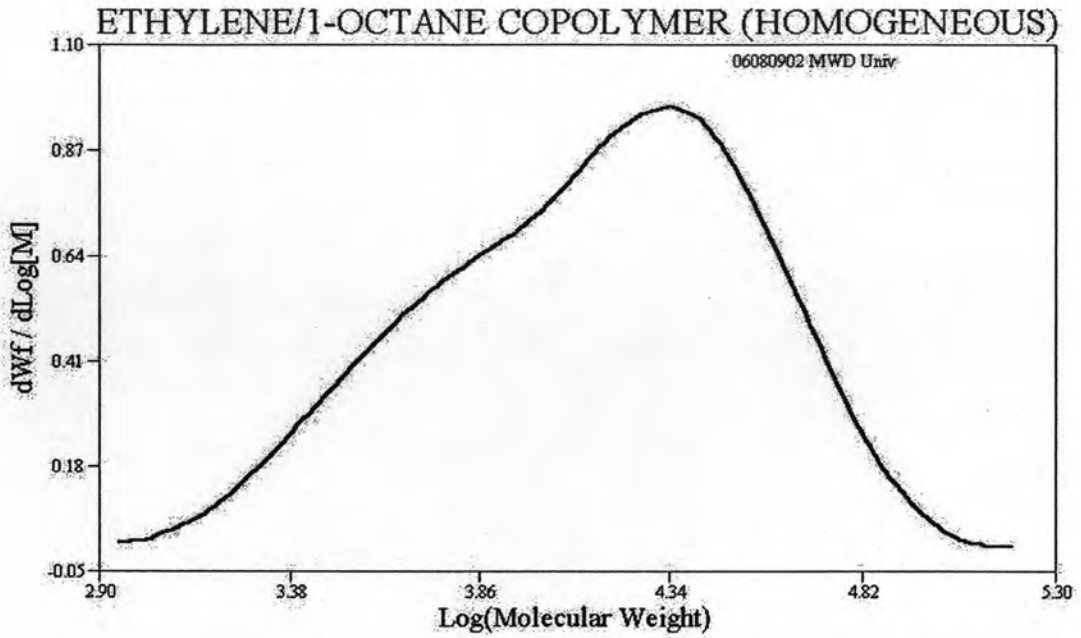

Figure C-1. GPC curve of ethylene/ 1-octene copolymerization produced with homogeneous

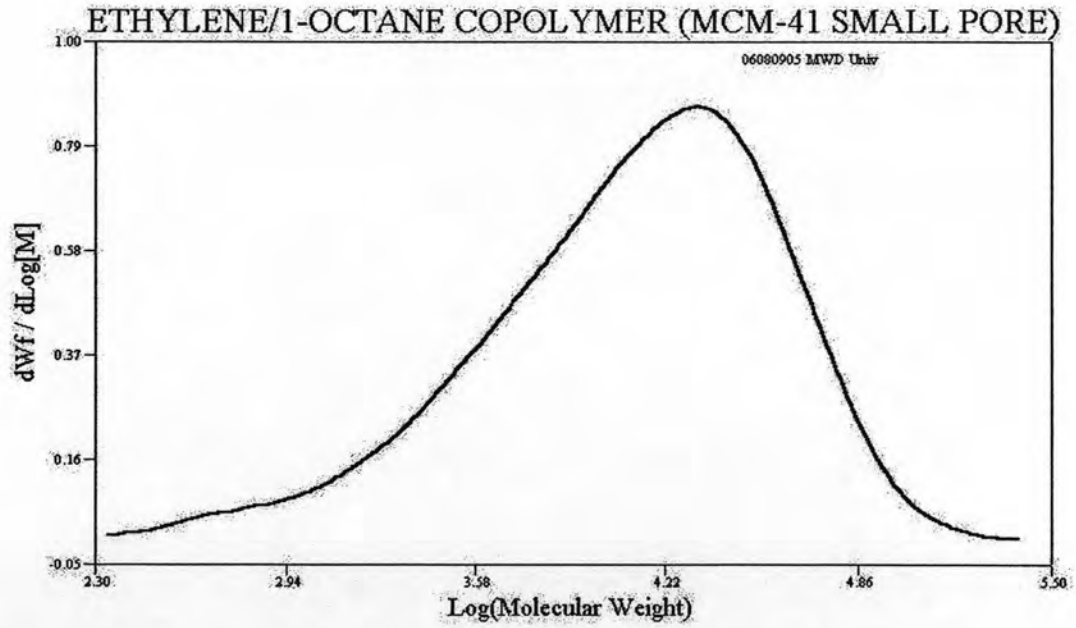

Figure C-2. GPC curve of ethylene/ 1-octene copolymerization produced with MCM-41 small pore

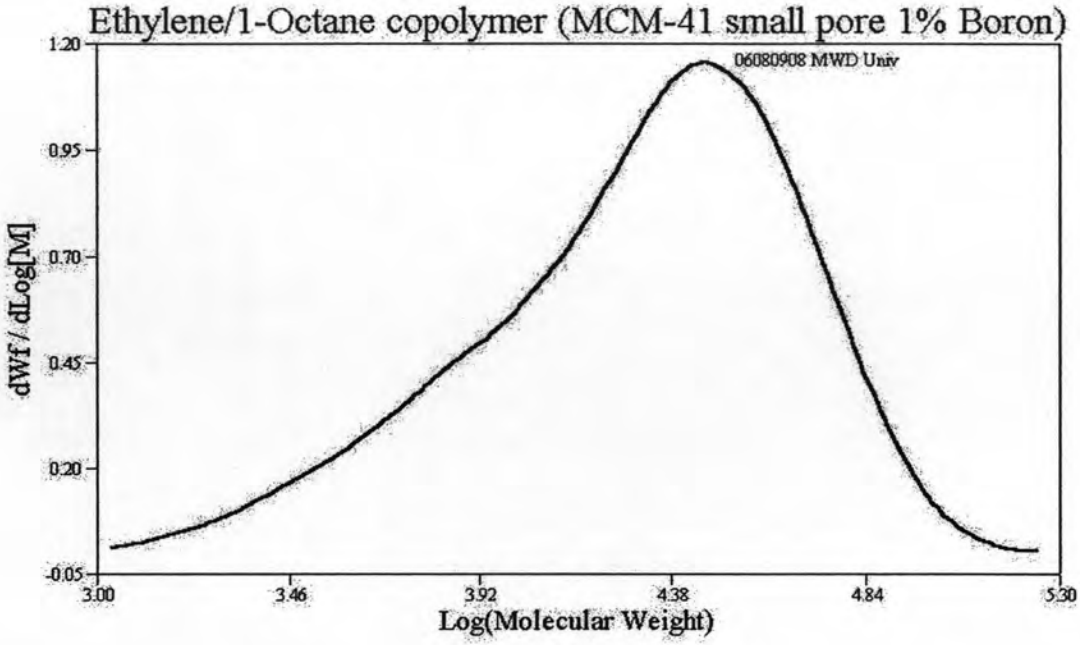

Figure C-3. GPC curve of ethylene/ 1-octene copolymerization produced with MCM-41 small pore via 1%wt of boron loading

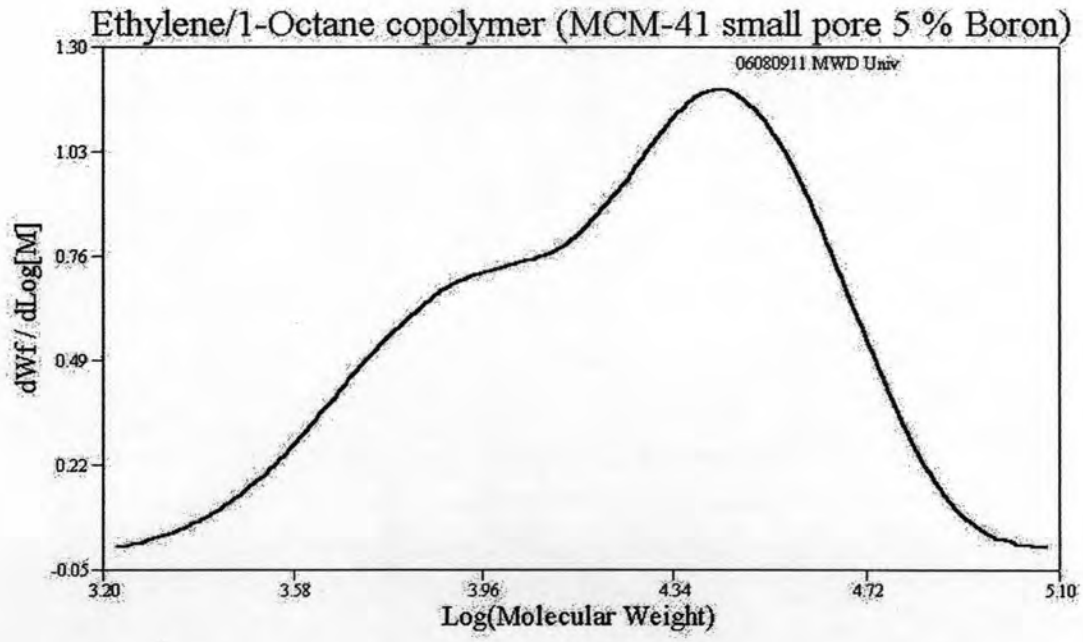

Figure C-4. GPC curve of ethylene/ 1-octene copolymerization produced with MCM-41 small pore via 5%wt of boron loading

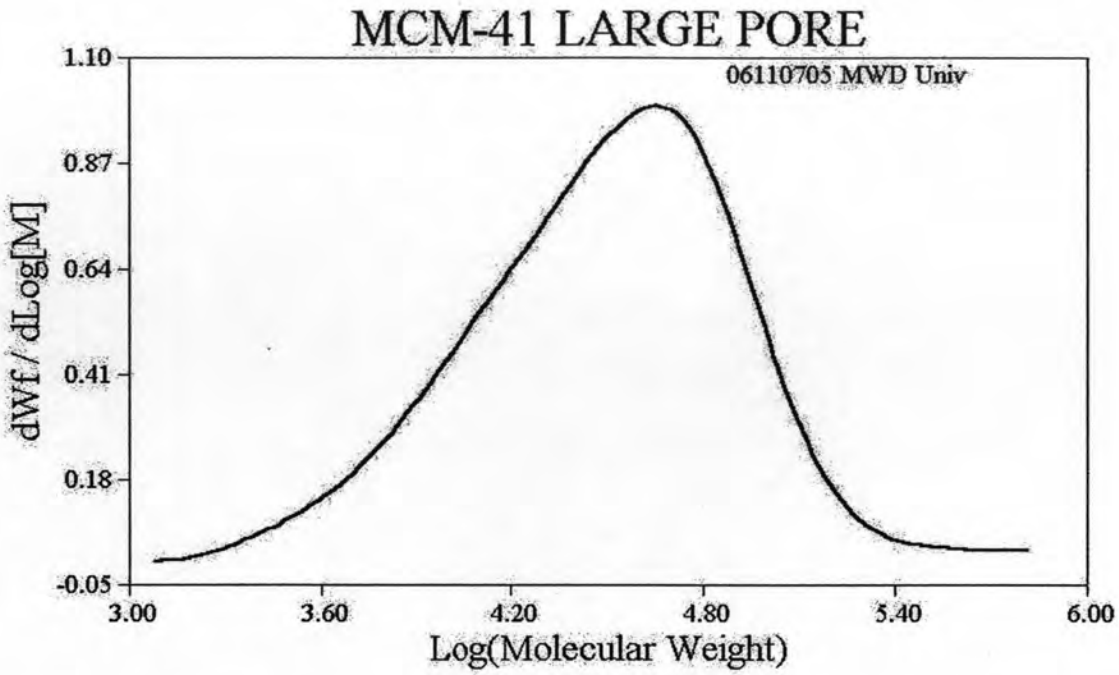

Figure C-5. GPC curve of ethylene/ 1-octene copolymerization produced with MCM-41 large pore

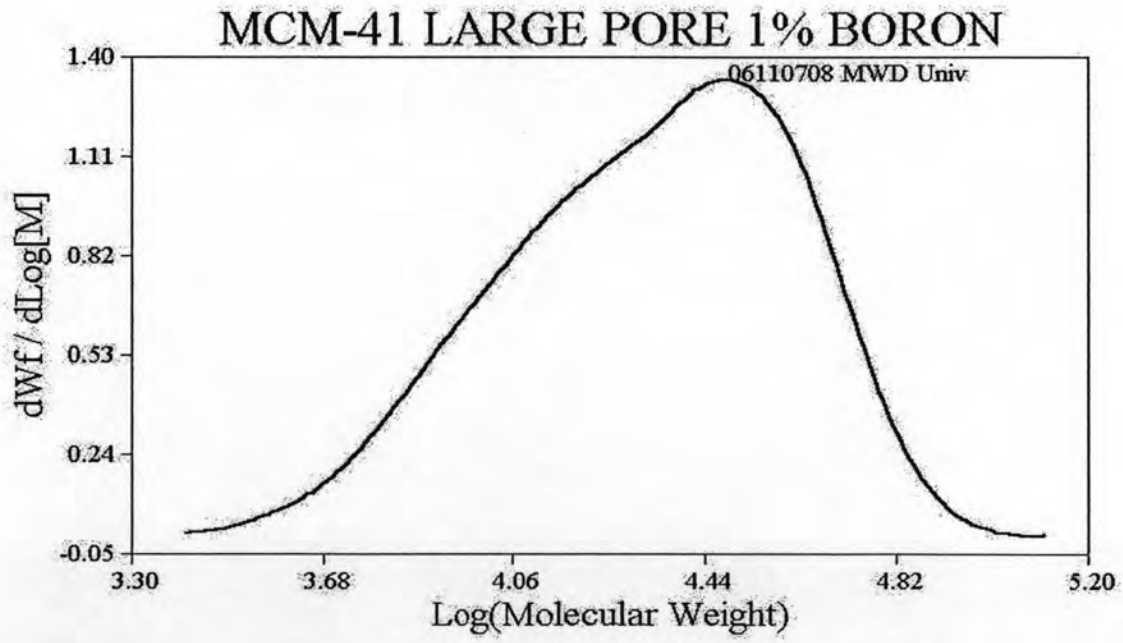

Figure C-6. GPC curve of ethylene/ 1-octene copolymerization produced with MCM-41 large pore via 1%wt of boron loading

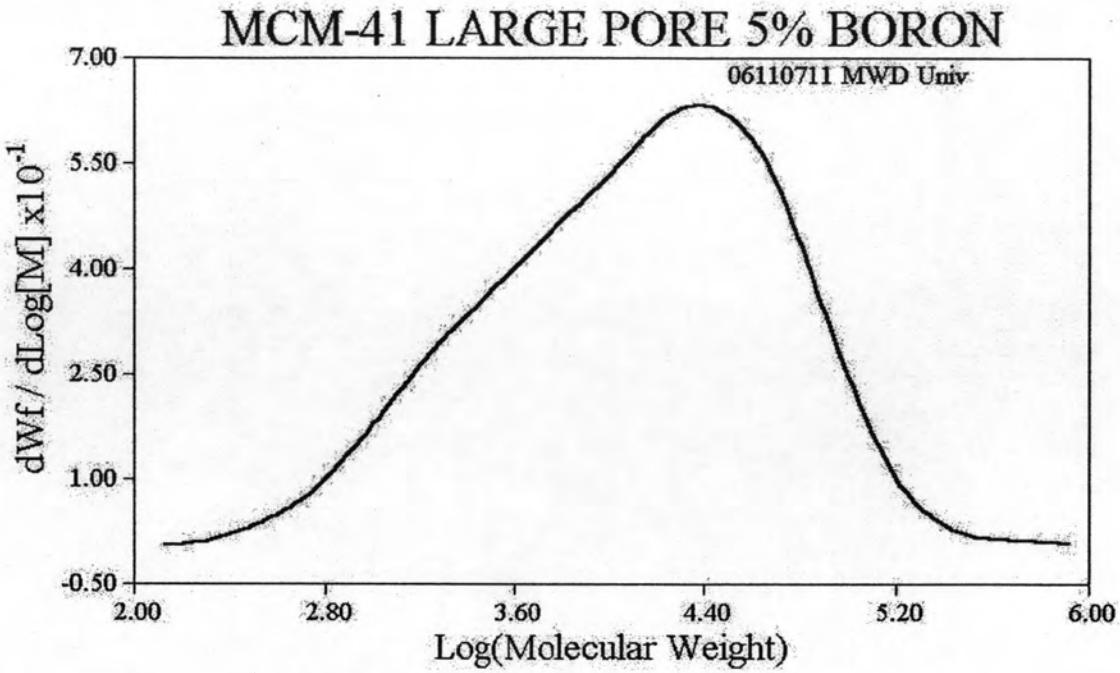

Figure C-7. GPC curve of ethylene/ 1-octene copolymerization produced with MCM-41 large pore via 5%wt of boron loading

APPENDIX D
(Energy Dispersive X-Ray Spectroscopy)

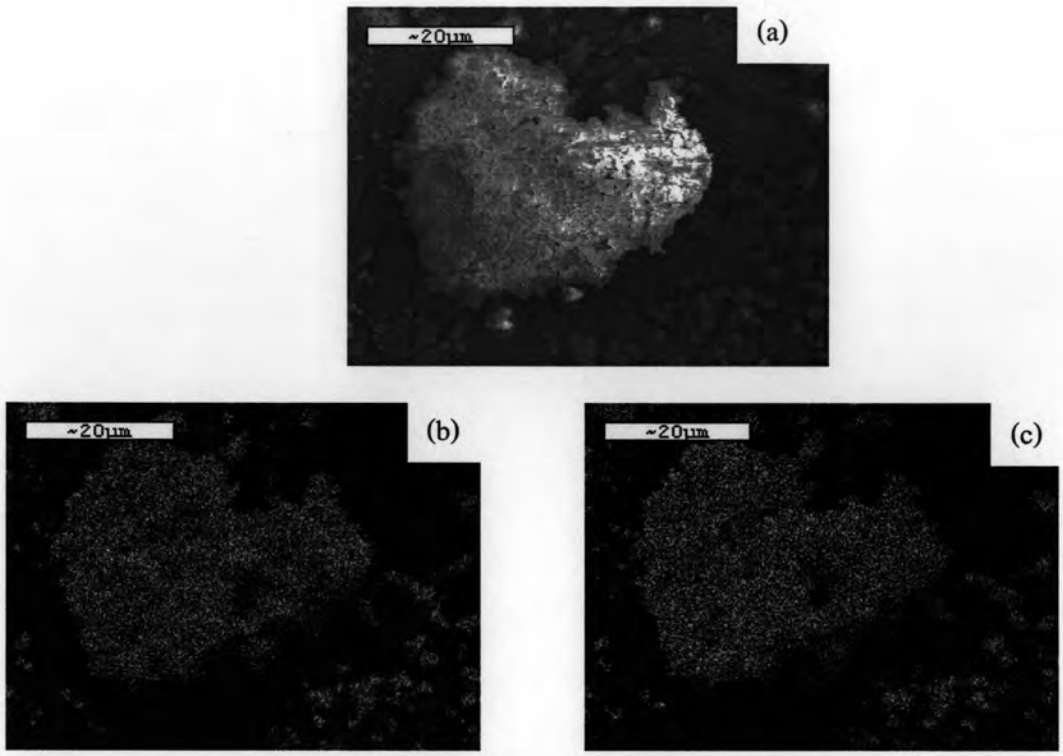

Figure D-1. EDX mapping of MCM-41 small pore scan no.1: (a) MCM-41 small pore; (b) Si-mapping of MCM-41 small pore; (c) Al-Mapping of MCM-41 small pore.

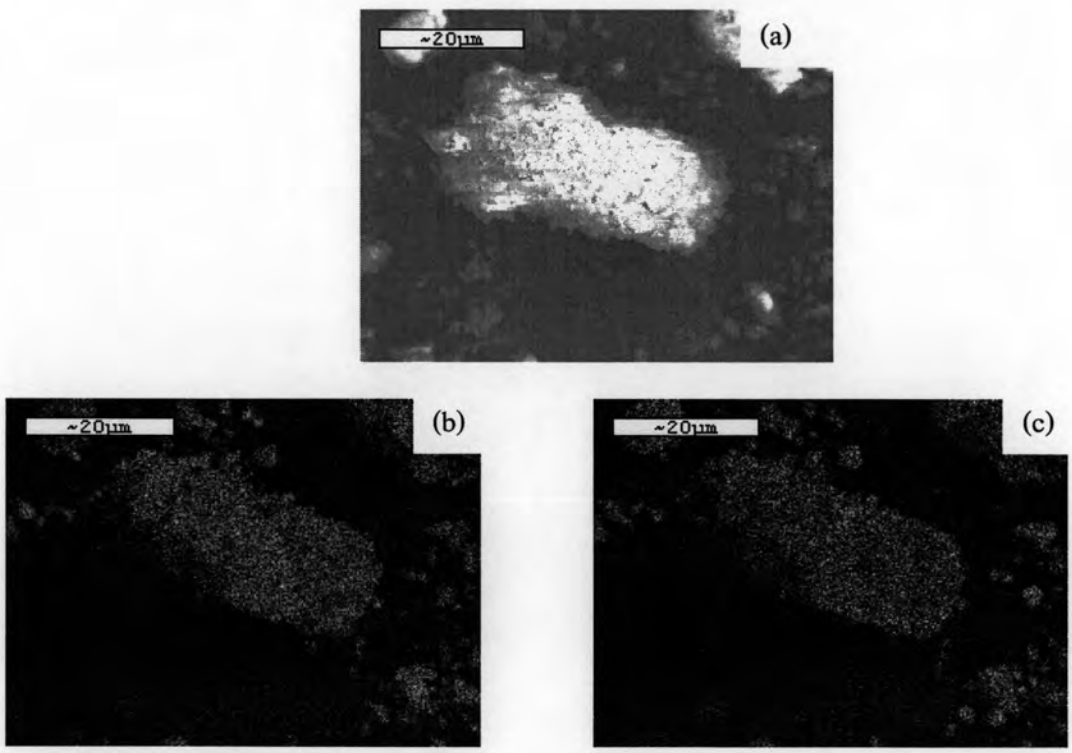

Figure D-2. EDX mapping of MCM-41 small pore scan no.2: (a) MCM-41 small pore; (b) Si-mapping of MCM-41 small pore; (c) Al-Mapping of MCM-41 small pore.

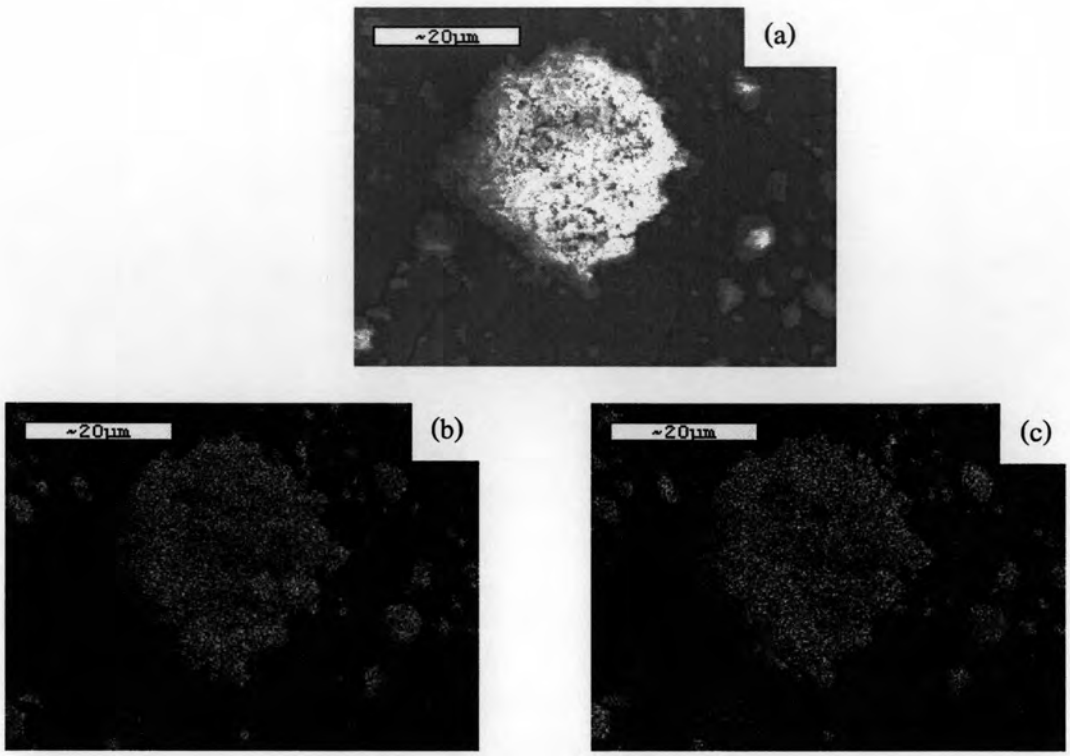

Figure D-3. EDX mapping of MCM-41 small pore scan no.3: (a) MCM-41 small pore; (b) Si-mapping of MCM-41 small pore; (c) Al-Mapping of MCM-41 small pore.

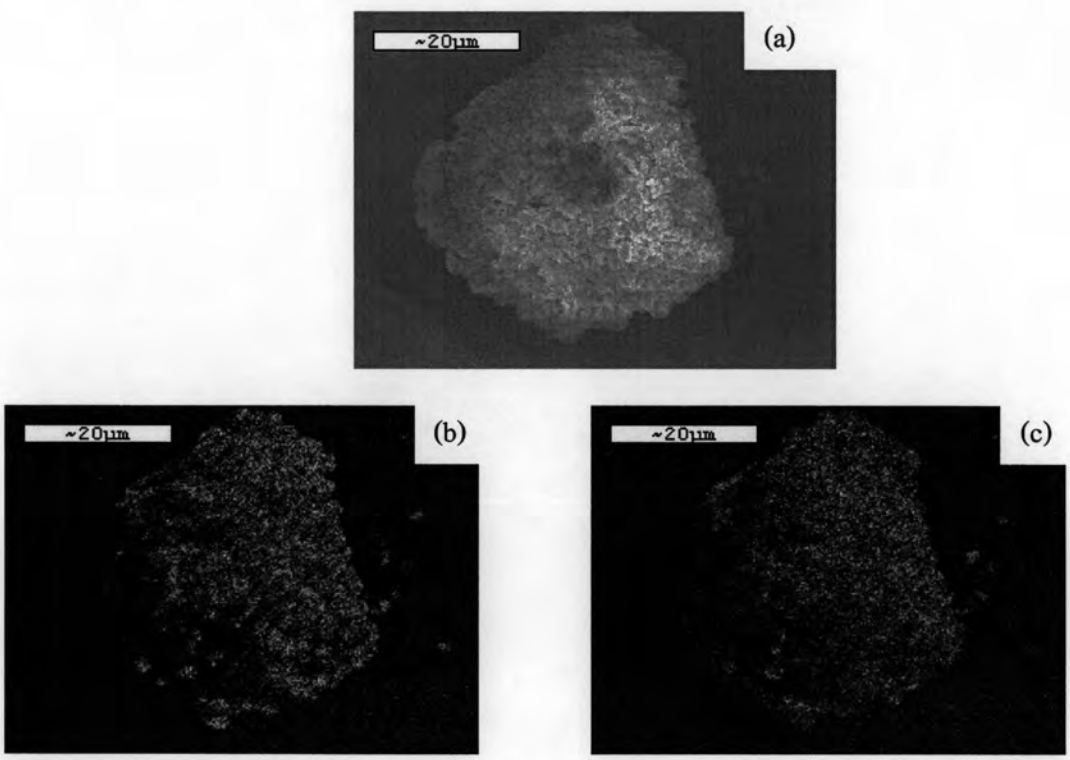

Figure D-4. EDX mapping of MCM-41 small pore1%B loading scan no.1: (a) 1B-MCM-41 small pore; (b) Si-mapping of 1B-MCM-41 small pore; (c) Al-Mapping of 1B-MCM-41 small pore.

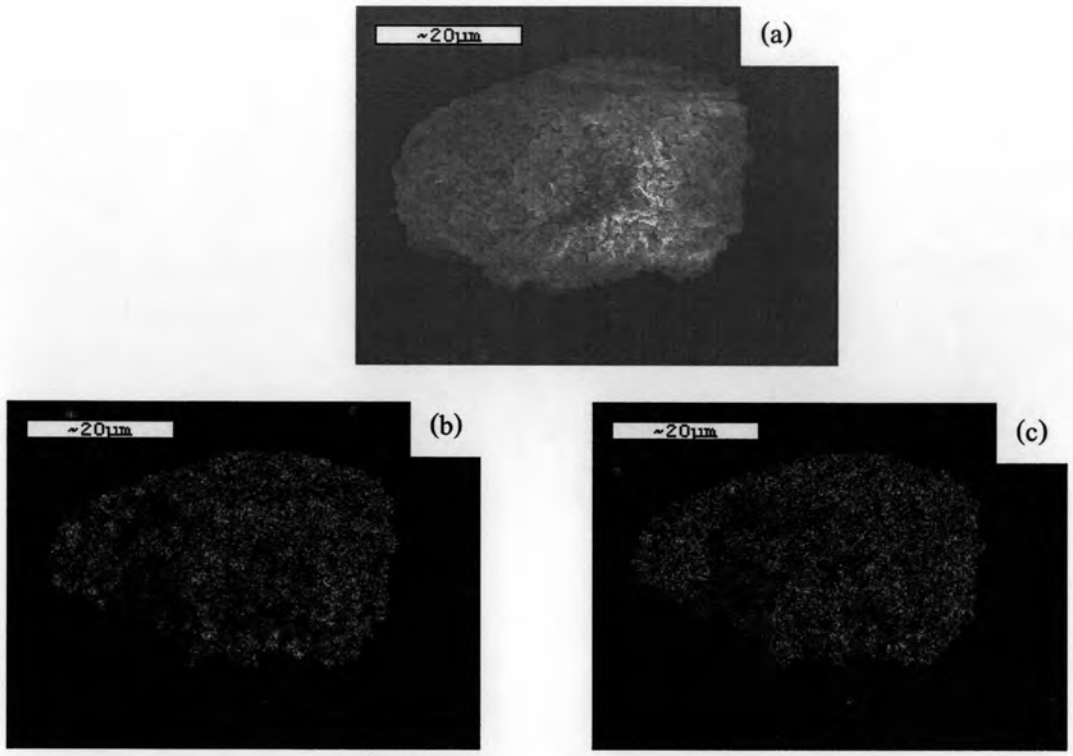

Figure D-5. EDX mapping of MCM-41 small pore1%B loading scan no.2: (a) 1B-MCM-41 small pore; (b) Si-mapping of 1B-MCM-41 small pore; (c) Al-Mapping of 1B-MCM-41 small pore.

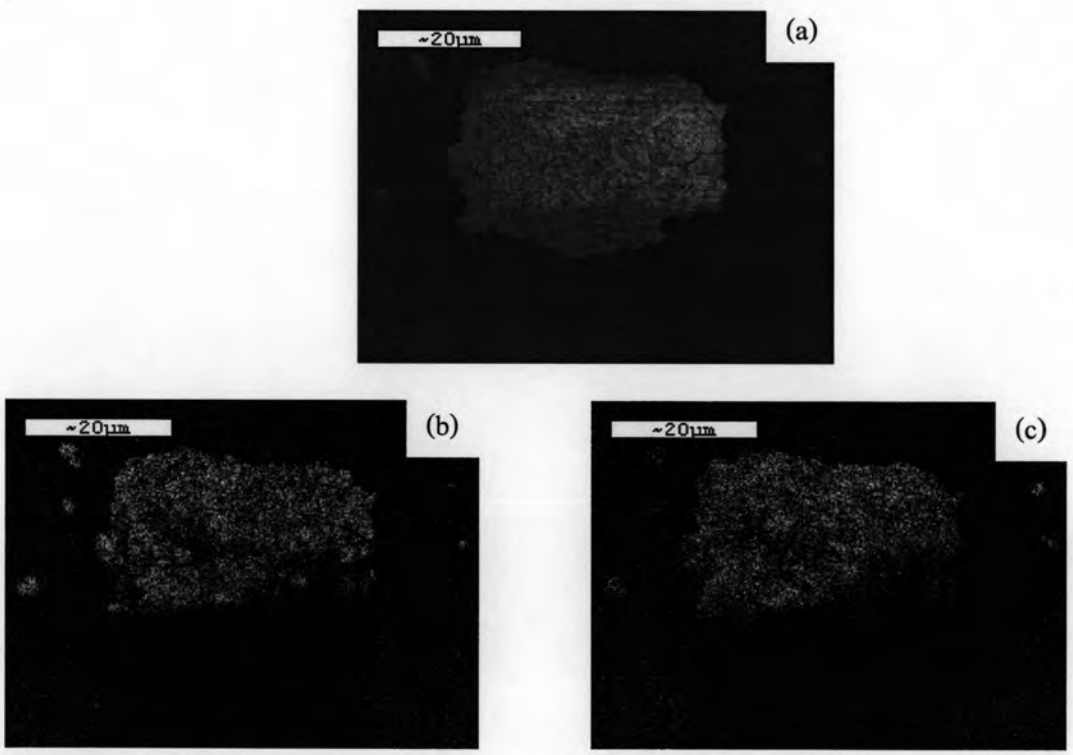

Figure D-6. EDX mapping of MCM-41 small pore1%B loading scan no.3: (a) 1B-MCM-41 small pore; (b) Si-mapping of 1B-MCM-41 small pore; (c) Al-Mapping of 1B-MCM-41 small pore.

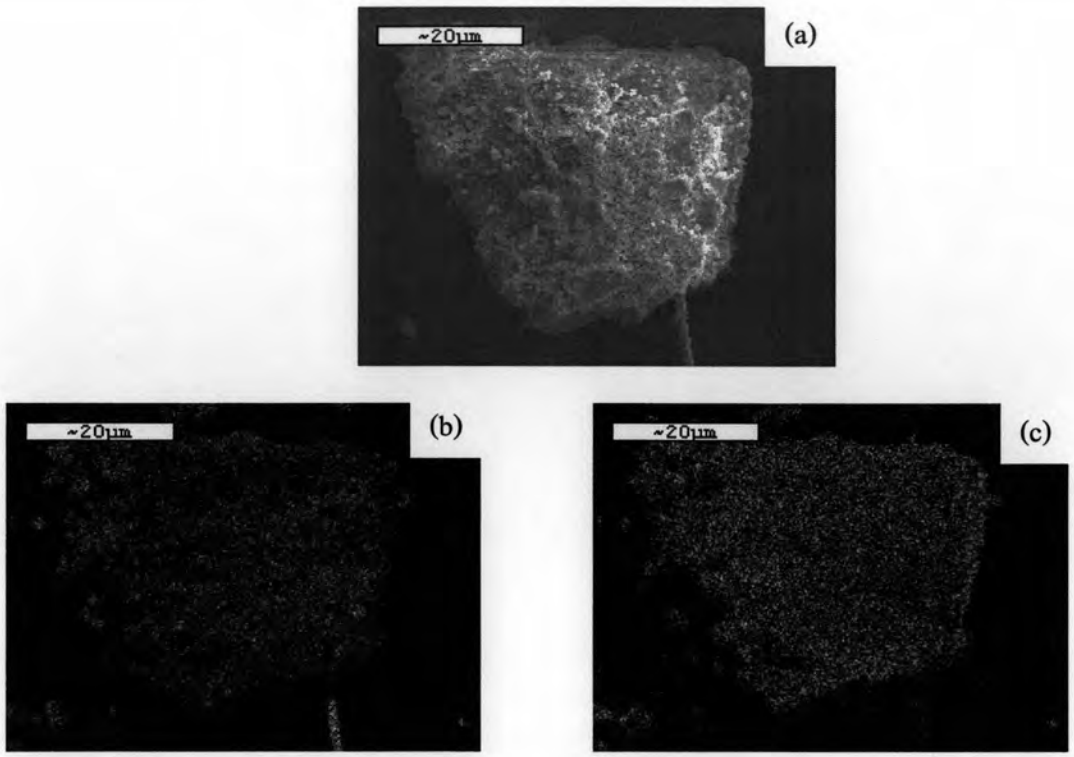

Figure D-7. EDX mapping of MCM-41 small pore5%B loading scan no.1: (a) 5B-MCM-41 small pore; (b) Si-mapping of 5B-MCM-41 small pore; (c) Al-Mapping of 5B-MCM-41 small pore.

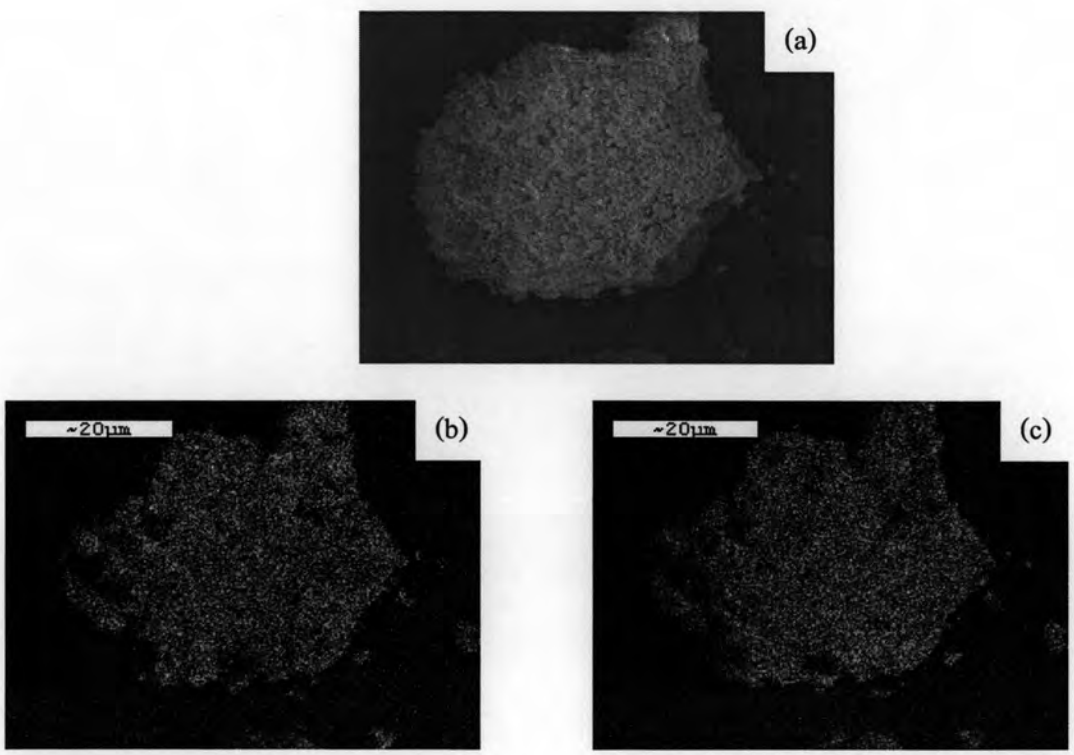

Figure D-8. EDX mapping of MCM-41 small pore5%B loading scan no.2: (a) 5B-MCM-41 small pore; (b) Si-mapping of 5B-MCM-41 small pore; (c) Al-Mapping of 5B-MCM-41 small pore.

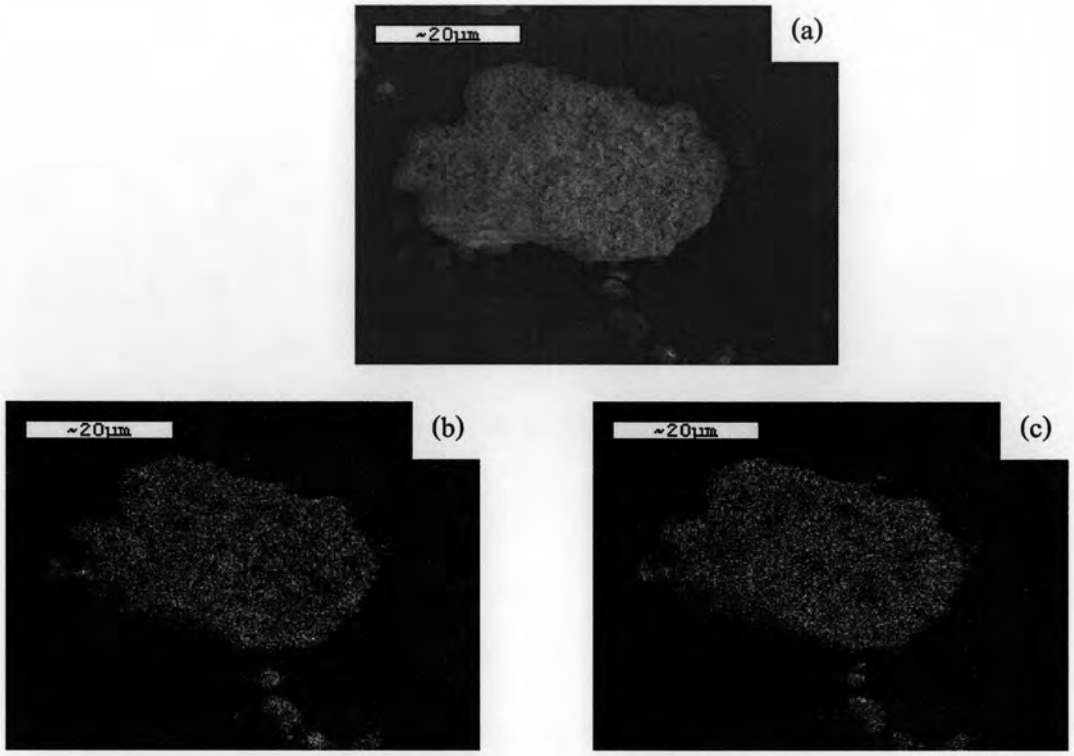

Figure D-9. EDX mapping of MCM-41 small pore5%B loading scan no.3: (a) 5B-MCM-41 small pore; (b) Si-mapping of 5B-MCM-41 small pore; (c) Al-Mapping of 5B-MCM-41 small pore.

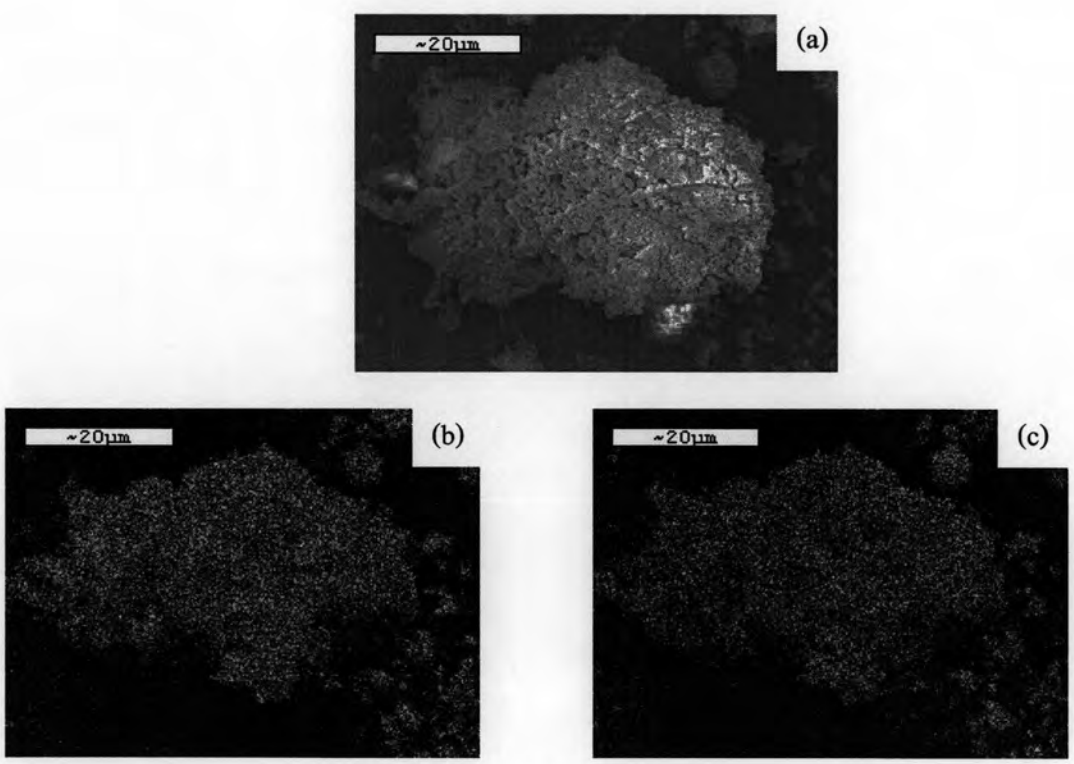

Figure D-10. EDX mapping of MCM-41 large pore scan no.1: (a) MCM-41 large pore; (b) Si-mapping of MCM-41 large pore; (c) Al-Mapping of MCM-41 large pore.

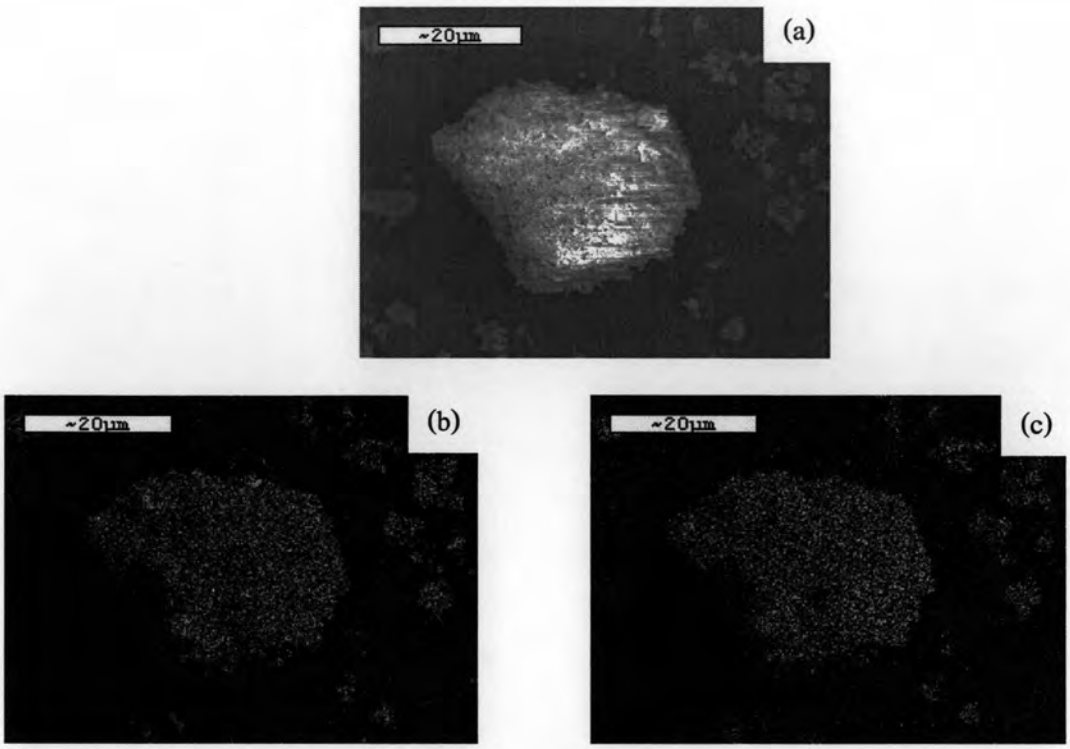

Figure D-11. EDX mapping of MCM-41 large pore scan no.2: (a) MCM-41 large pore; (b) Si-mapping of MCM-41 large pore; (c) Al-Mapping of MCM-41 large pore.

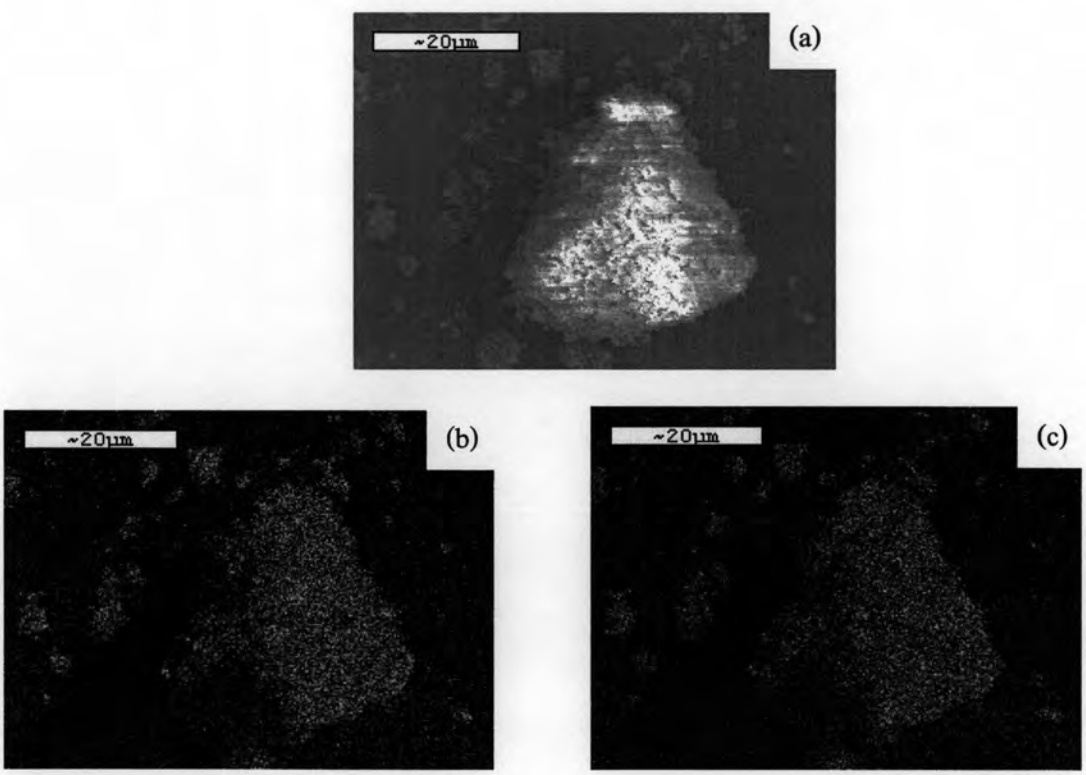

Figure D-12. EDX mapping of MCM-41 large pore scan no.3: (a) MCM-41 large pore; (b) Si-mapping of MCM-41 large pore; (c) Al-Mapping of MCM-41 large pore.

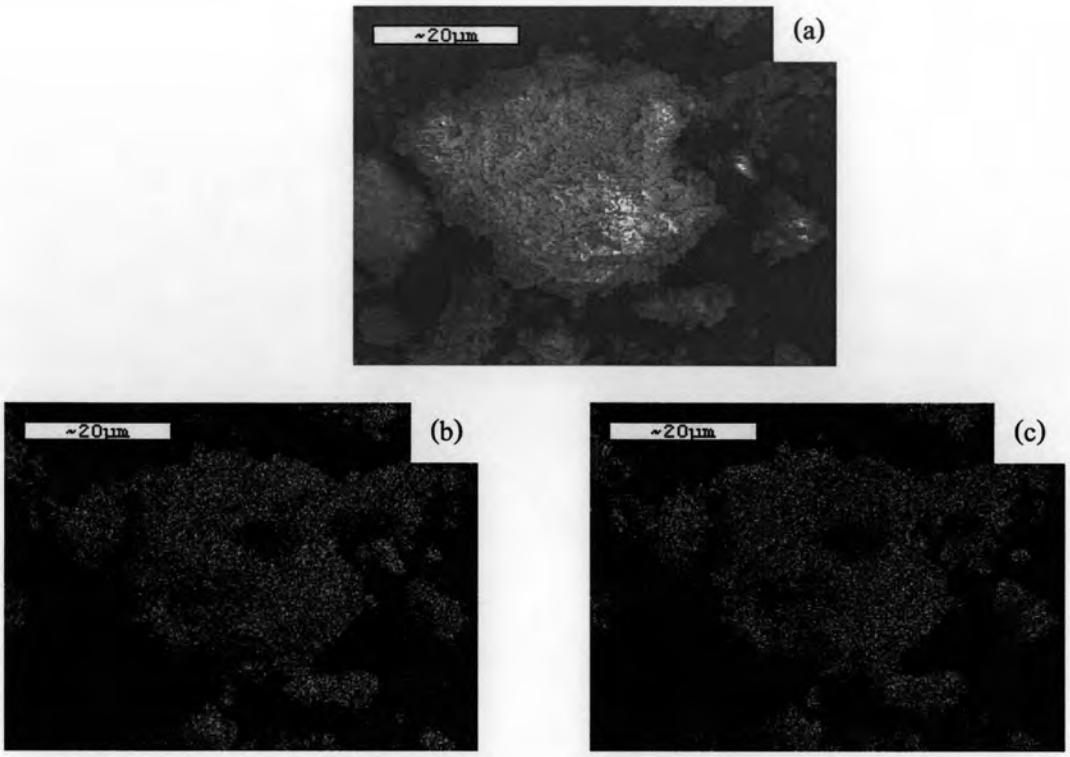

Figure D-13. EDX mapping of MCM-41 large pore1%B loading scan no.1: (a) 1B-MCM-41 large pore; (b) Si-mapping of 1B-MCM-41 large pore; (c) Al-Mapping of 1B-MCM-41 large pore.

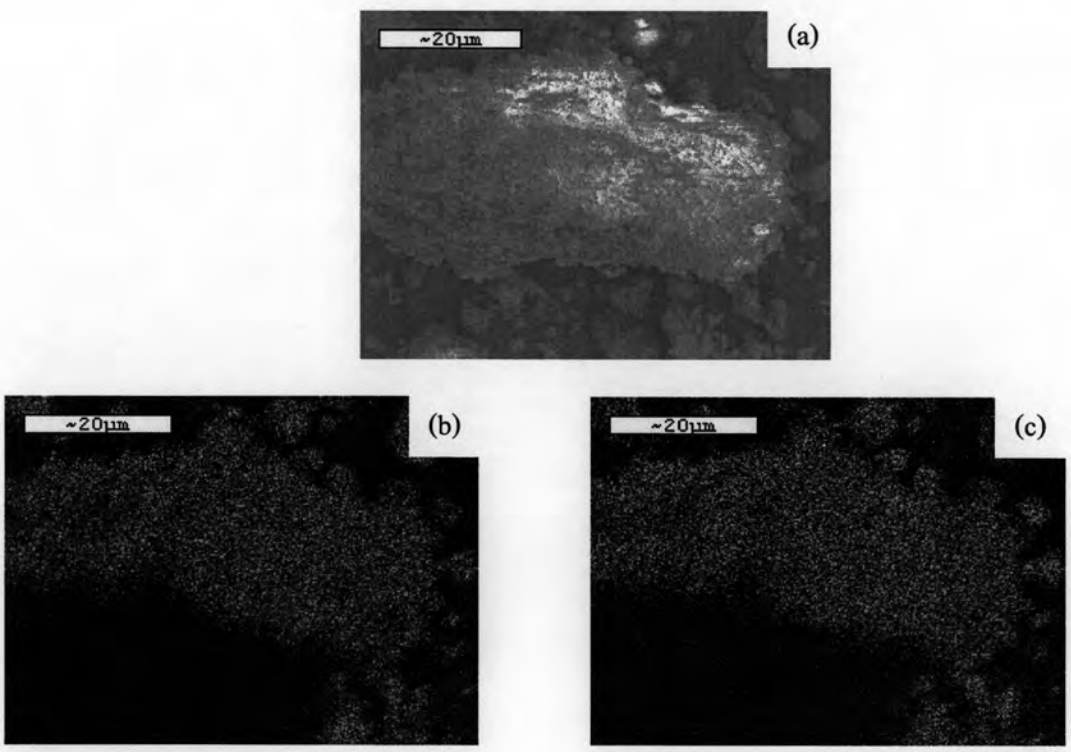

Figure D-14. EDX mapping of MCM-41 large pore1%B loading scan no.2: (a) 1B-MCM-41 large pore; (b) Si-mapping of 1B-MCM-41 large pore; (c) Al-Mapping of 1B-MCM-41 large pore.

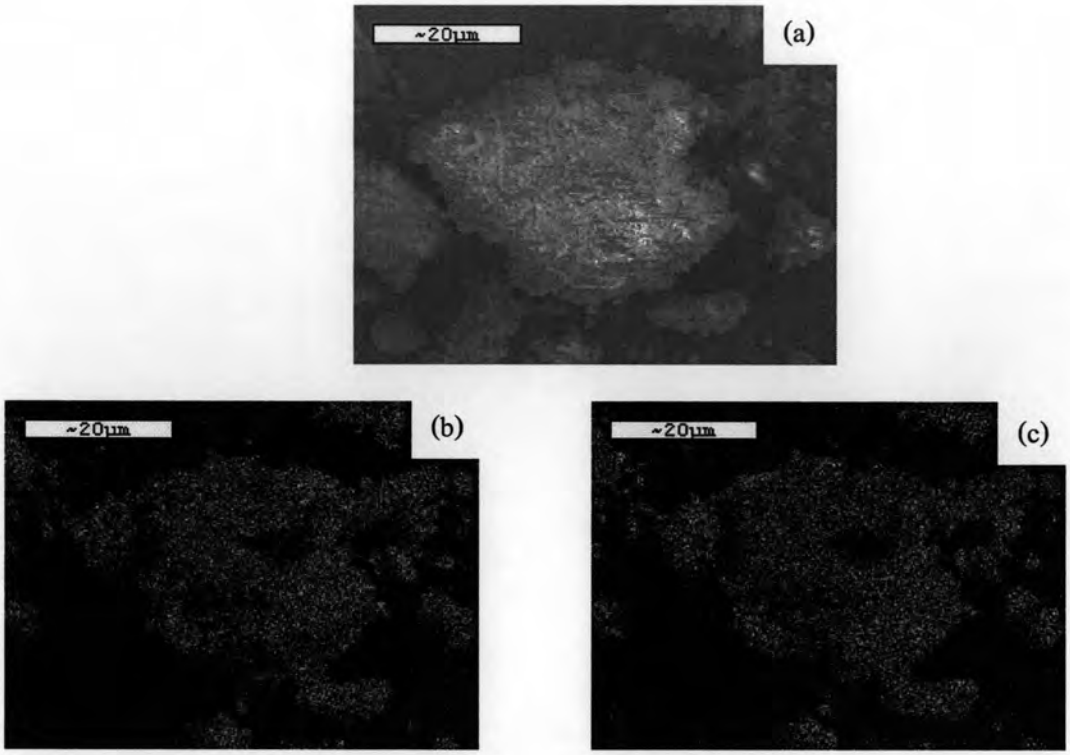

Figure D-15. EDX mapping of MCM-41 large pore1%B loading scan no.3: (a) 1B-MCM-41 large pore; (b) Si-mapping of 1B-MCM-41 large pore; (c) Al-Mapping of 1B-MCM-41 large pore.

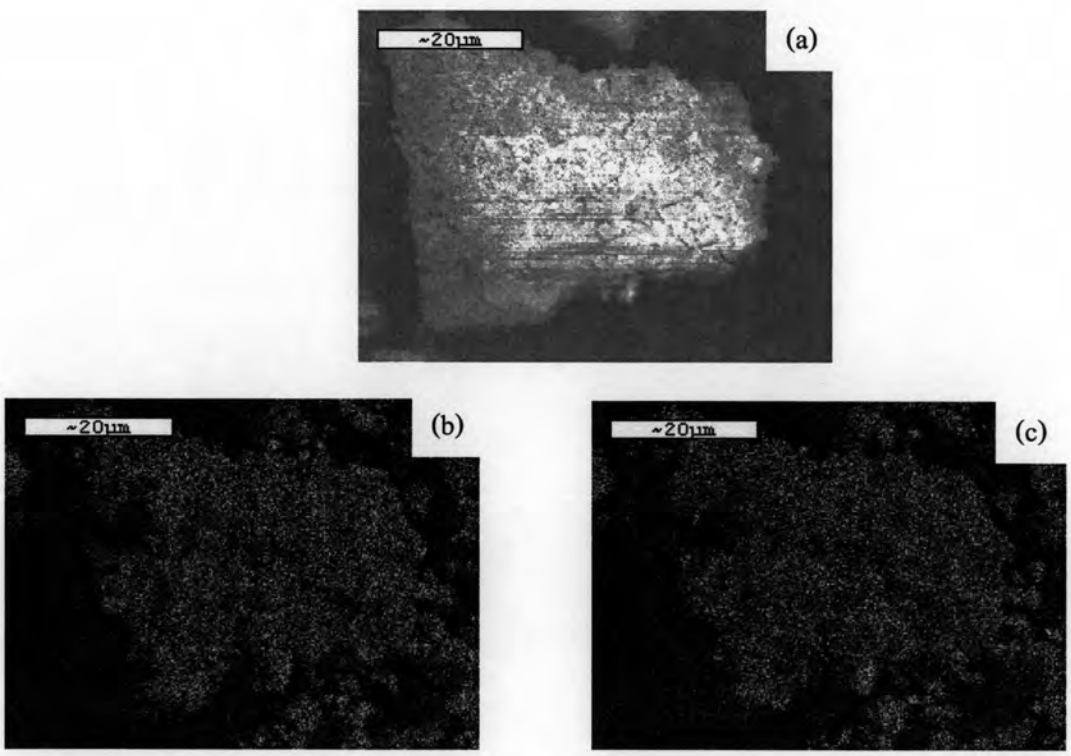

Figure D-16. EDX mapping of MCM-41 large pore5%B loading scan no.1: (a) 5B-MCM-41 large pore; (b) Si-mapping of 5B-MCM-41 large pore; (c) Al-Mapping of 5B-MCM-41 large pore.

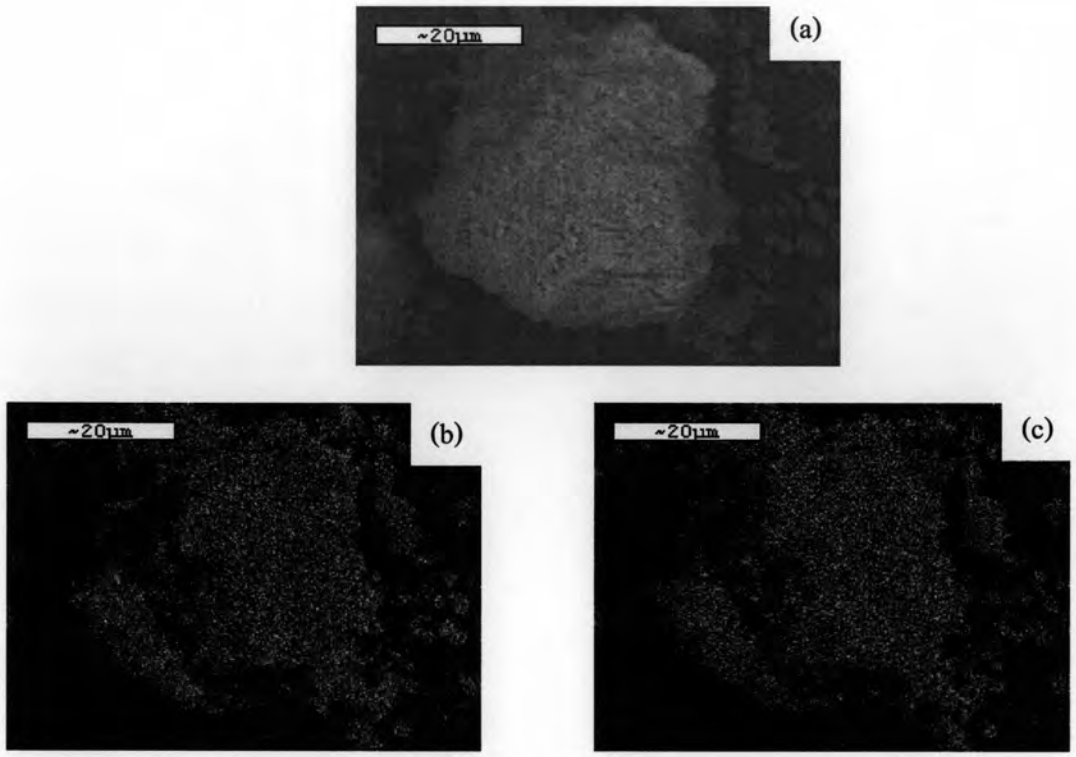

Figure D-17. EDX mapping of MCM-41 large pore5%B loading scan no.2: (a) 5B-MCM-41 large pore; (b) Si-mapping of 5B-MCM-41 large pore; (c) Al-Mapping of 5B-MCM-41 large pore.

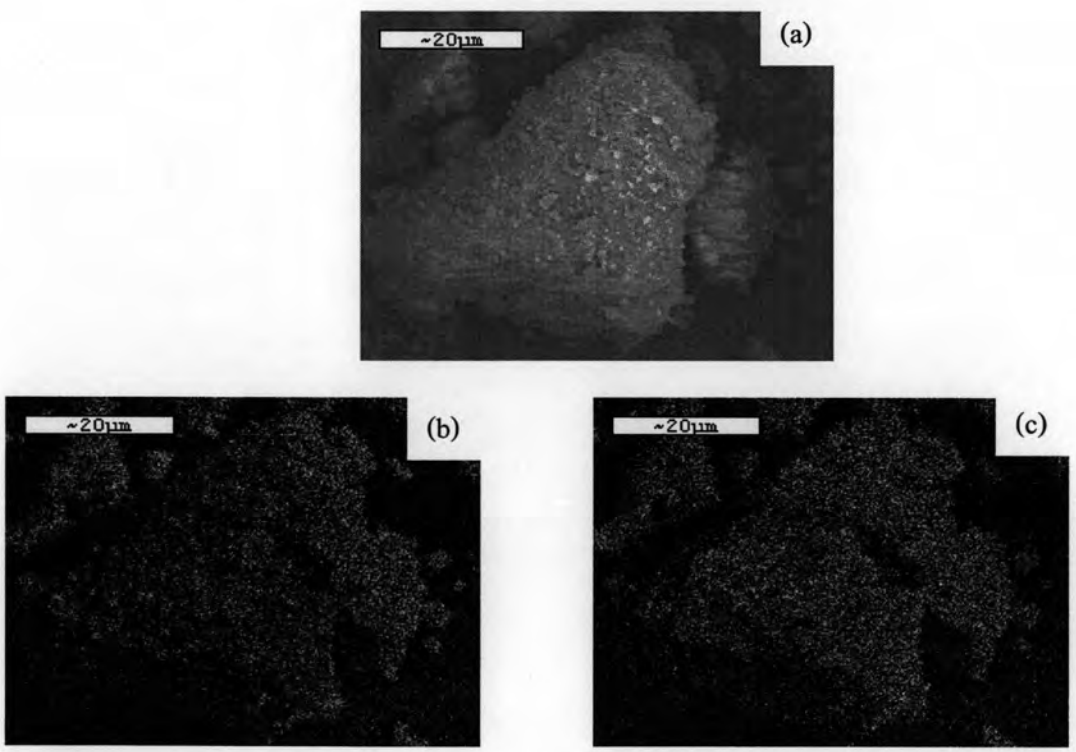

Figure D-18. EDX mapping of MCM-41 large pore5%B loading scan no.3: (a) 5B-MCM-41 large pore; (b) Si-mapping of 5B-MCM-41 large pore; (c) Al-Mapping of 5B-MCM-41 large pore.

APPENDIX E
(Calculation of Polymer Properties)

E.1 Calculation of polymer microstructure

Polymer microstructure and also triad distribution of monomer can be calculated according to the Galland G.B. [64].The detail of calculation was be interpreted as follow:

E.1.1 Ethyelene/1-octene copolymer

The integral area of ^{13}C-NMR spectrum in the specify range are listed.

T_A	=	39.5 - 42	ppm
T_B	=	38.1	ppm
T_C	=	36.4	ppm
T_D	=	33 - 36	ppm
T_E	=	32.2	ppm
T_F	=	28.5 - 31	ppm
T_G	=	25.5 - 27.5	ppm
T_H	=	24 - 25	ppm
T_I	=	22 - 23	ppm
T_J	=	14 – 15	ppm

Triad distribution was calculated as the followed formula

[OOO] =	$T_A - 0.5T_C$
[EOO] =	T_C
[EOE] =	T_B
[EEE] =	$0.5T_F - 0.25T_E - 0.25T_G$
[OEE] =	$T_G - T_E$
[OEO] =	T_H

All copolymer was calculated for the relative comonomer reactivity (r_E for ethylene and r_C for the commoner) by using the general formula below:

$r_E = 2[EE]/([EC]X)$ $\qquad$ $r_C = 2[CC]X/[EC]$

where r_E = ethylene reactivity ratio

r_C = comonomer (α-olefin) reactivity ratio

[EE] = [EEE] + 0.5[CEE]

[EC] = [CEC] + 0.5[CEE] + [ECE] + 0.5[ECC]

[CC] = [CCC] + 0.5[ECC]

X = [E]/[C] in the feed = concentration of ethylene (mol/L) / concentration of comonomer (mol/L) in the feed.

E.2 Calculation of crystallinity for ethylene/α-olefin copolymer

The crystallinities of copolymers were determined by differential scanning calorimeter. %crystallinity of copolymers is calculated from equationn [66].

$$\chi(\%) = \frac{\Delta H_m}{\Delta H_m^0} \times 100$$

Where $\chi(\%)$ = %crystallinity

ΔH_m = the heat of fusion of sample (J/g)

ΔH_m^0 = the heat of fusion of perfectly crystalline polyethylene (286 J/g) [66]

APPENDIX F
(X-ray Photoelectron Spectroscopy)

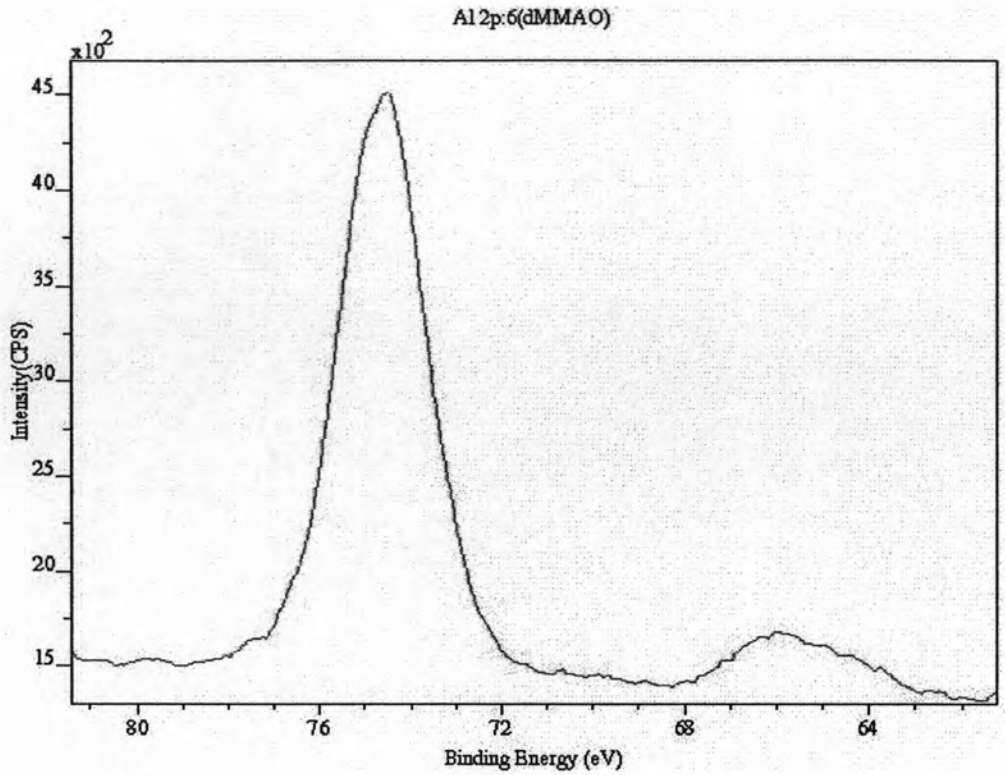

Figure F-1. Binding energy for Al 2p of dMMAO

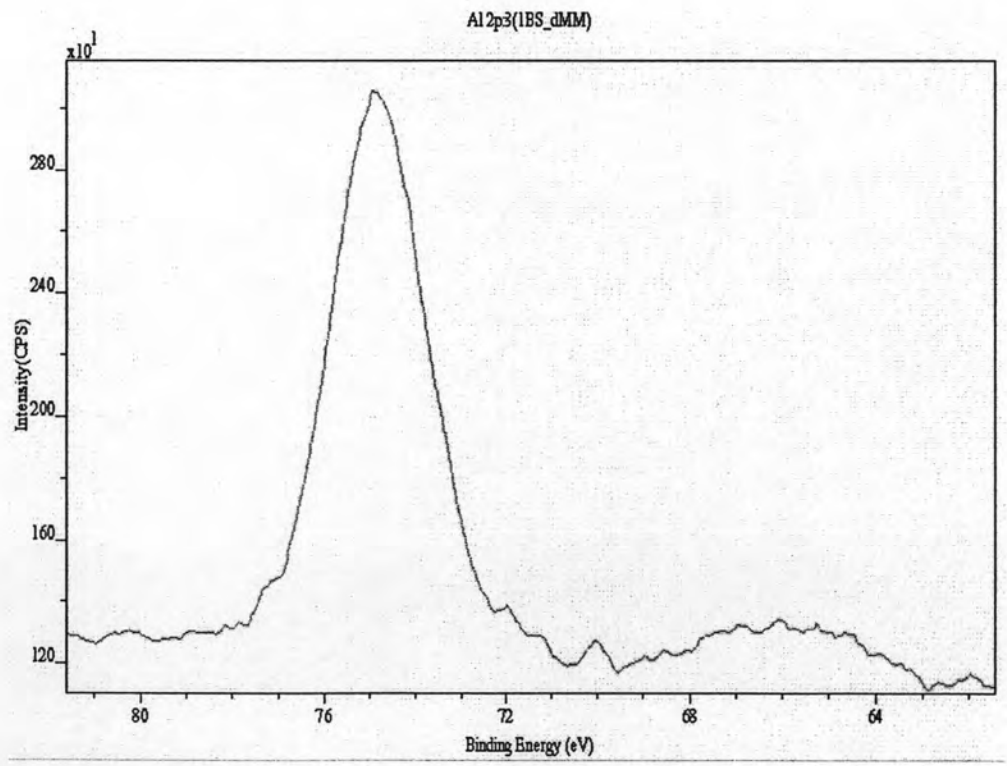

Figure F-2. Binding energy for Al 2p of MCM-41 small pore with 1 wt% of B loading

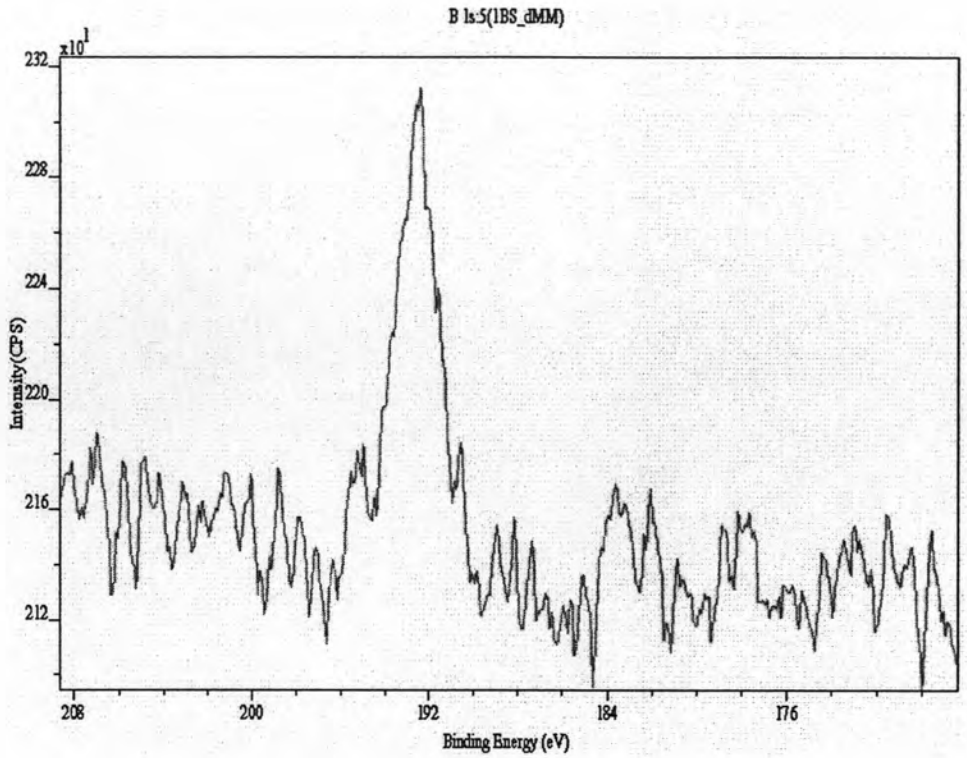

Figure F-3. Binding energy for B 1s of MCM-41 small pore with 1 wt% of B loading

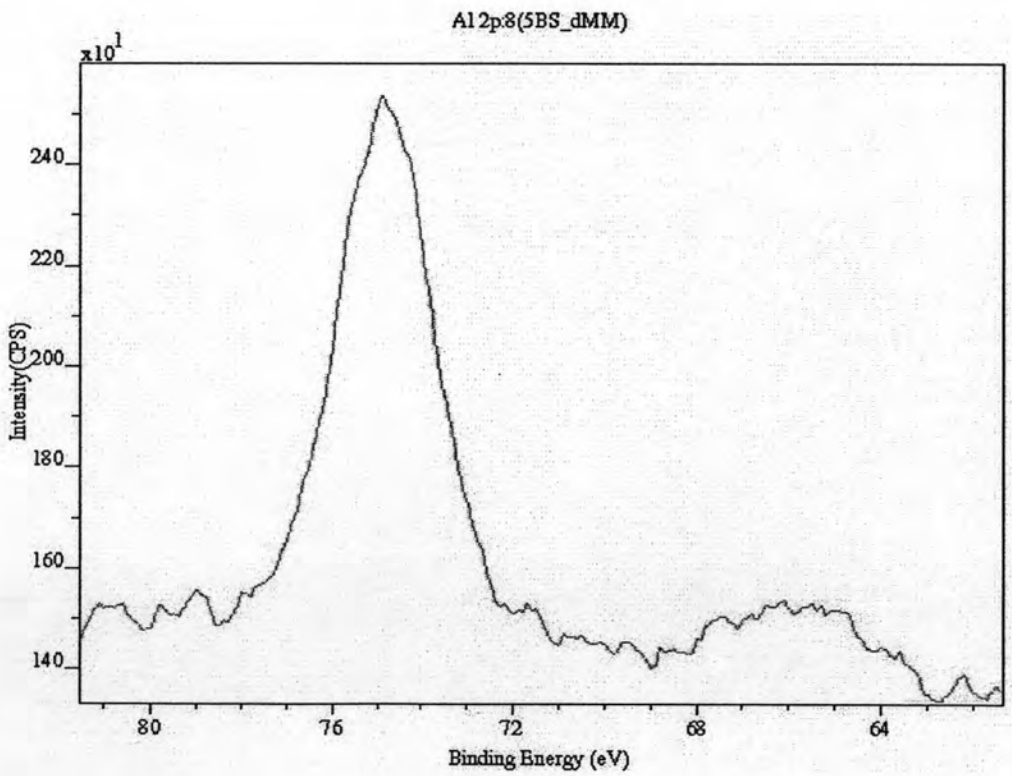

Figure F-4. Binding energy for Al 2p of MCM-41 small pore with 5 wt% of B loading

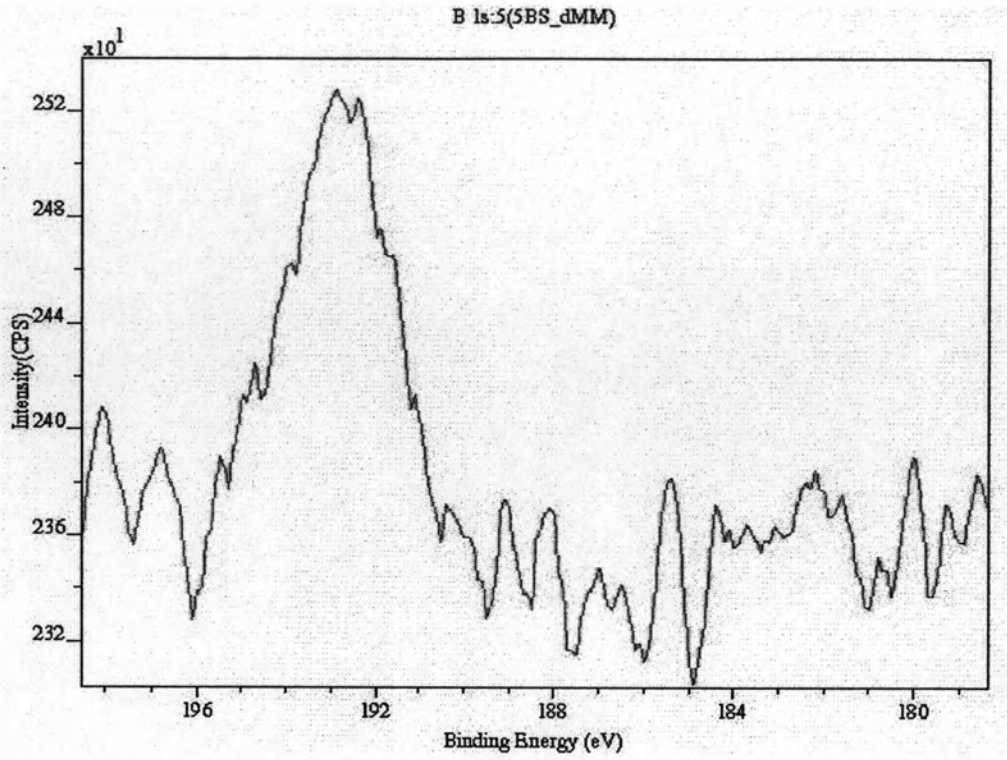

Figure F-5. Binding energy for B 1s of MCM-41 small pore with 5 wt% of B loading

APPENDIX G
(The Submitted Paper to Industrial Engineering Chemistry Resource)

Effect of boron-modified MCM-41-supported dMMAO/zirconocene catalyst on copolymerization of ethylene/1-octene for LLDPE synthesis

Supaluk Jiamwijitkul, Bunjerd Jongsomjit* and Piyasan Praserthdam

Center of Excellence on Catalysis and Catalytic Reaction Engineering
Department of Chemical Engineering, Faculty of Engineering
Chulalongkorn University, Bangkok 10330 Thailand

Abstract

In this work, the boron (B) modification on MCM-41-supported dMMAO/zirconocene catalysts showed a promising increase (almost 2 times) in catalytic activity for ethylene/1-octene copolymerization. Enhanced activity can be attributed to the decreased interaction between the support and dMMAO with B modification as proven by TGA. It was proposed that B acted as a spacer to anchor the support and dMMAO. However, at high B loading (ca. 5 wt%), the activity slightly decreased due to the migration of dMMAO into B layer resulting in less surface concentration of $[Al]_{dMMAO}$ as measured by XPS. The inhibition of chain transfer reaction during polymerization apparently occurred upon the B modification indicating higher MW of polymer. It was also suggested that B modification rendered more uniform catalytic sites leading to narrow MWD of polymer observed.

Keywords: MCM-41; B-modification; metallocene catalyst; copolymerization; polyolefins

*Corresponding author, **E-mail:** bunjerd.j@chula.ac.th

Tel: 662-2186869, **Fax:** 662-2186877

1. Introduction

During the past years, metallocene catalysts have brought great impact on both in academia and polymer industry. Metallocene catalysts have revolutionized olefin polymerization catalysis because of the tailor-made polymer properties. They provide high activity with narrow molecular weight distribution (MWD) when compared to the conventional Ziegler-Natta (ZN) catalysts. Furthermore, they also produce a very uniform polymer due to their single-site catalytic nature. However, it was found that the homogeneous metallocene catalytic systems have two major disadvantages: the lack of morphology control of polymer causing the reactor fouling and the limitation of being able to use only in the solution process whereas the existing technologies are mainly based on gas phase and slurry processes. Therefore, binding these metallocene catalysts onto inorganic supports can provide a promising way to overcome these drawbacks.

In general, the heterogeneous metallocene catalytic system (or supported system) apparently has a lower activity than its corresponding homogeneous one at similar conditions. However, it is able to control the polymer morphology due to the support employed, and then avoid the fouling effect, the sticking of formed polymer to the reactor wall.[1] Supported metallocene catalysts are widely used in the olefin polymerization.[2-12] Some scientists have carried out the polymerization using the regular arranged mesoporous silica materials such as MCM-41 as the support of metallocene catalysts.[13, 14] Since their discovery in 1992,[15] MCM-41 and related mesoporous molecular sieves have attracted much attention. As known, MCM-41 possesses unidirectional, channel-like pores of rather uniform size, which are arranged in a regular hexagonal pattern. The pore diameters are adjustable in the range 15 to 100 Å depending on the synthesis conditions.[16] Many scientists investigated MCM-41 materials in which a catalytically active component was introduced. Several elements, such as Al [3, 4] and B[17-19] have been incorporated into the framework in order to generate potential catalytic activity. Therefore, a modification of the MCM-41 could provide an alternative strategy to obtain suitable supports to maintain high activity as in the homogeneous system for the supported metallocene catalysts.

In this present study, effect of B modification on MCM-41-supported dMMAO/zirconocene catalyst during ethylene/1-octene copolymerization was

investigated. The amounts of B loading were also varied. The characterization of different supports was performed by means of XRD, Raman spectroscopy and XPS. The polymer obtained was further analyzed using GPC in order to determine the effect of B modification on molecular weight (MW) and MWD.

2. Experimental section

2.1 Materials

All chemicals and polymerization were manipulated under an argon atmosphere, using a glove box and/or Schlenk techniques. Toluene was dried over dehydrated $CaCl_2$ and distilled over sodium/benzophenone before use. The *rac*-ethylenebis (indenyl) zirconium dichloride (*rac*-Et[Ind]$_2$ZrCl_2) was supplied from Aldrich Chemical Company, Inc. Modified methylaluminoxane (MMAO) in hexane was donated by Tosoh (Akso, Japan). Trialkylaluminum (TMA, 2 M in toluene) was supplied by Nippon Aluminum Alkyls, Ltd., Japan. Ultrahigh purity argon was further purified by passing it through columns that were packed with BASF catalyst R3-11G (molecular-sieved to 3 Å), sodium hydroxide (NaOH), and phosphorus pentaoxide (P_2O_5) to remove traces of oxygen and moisture. Ethylene gas (99.96% pure) was donated by National Petrochemical Co., Ltd., Thailand. 1-Octene (d = 0.715) was purchased from Aldrich Chemical Company, Inc.

2.2 Preparation of MCM-41 support

The MCM-41 support was synthesized according to the method described by Panpranot et al.[20] using the gel composition of CTABr : 0.3 NH_3 : 4 SiO_2 : Na_2O : 200 H_2O, where CTABr denotes cetyltrimethyl ammonium bromide. Briefly, 20.03 g of colloidal silica Ludox HS 40 % (Aldrich Chemical Company, Inc.) was mixed with 22.67 g of 11.78 % sodium hydroxide solution. Another mixture comprised of 12.15 g of CTABr (Aldrich Chemical Company, Inc.) in 36.45 g of deionized water, and 0.4 g of an aqueous solution of 25 % NH_3. Both of these mixture were stirred by agitator for 30 min, then heated statically at 373 K for 5 days. The obtained solid material was filtered, washed with deionized water until no base was detected and then dried at 373 K. The sample was then calcined in flowing nitrogen up to 823 K (1-2 K/min), then in air at the

same temperature for 5 h. After preparation, the MCM-41 support having the pore diameter of 3 nm and surface area of 864 m^2/g was obtained.

2.3 Preparation of B-modified MCM-41 support

B-modified MCM-41 supports were prepared by the incipient wetness impregnation on the support. The desired amount of the aqueous solution of boric acid (99.99% H_3BO_3, Aldrich Chemical Company, Inc.) was added onto the support to yield a final loading of approximately 1 and 5 wt% of B. The supports were dried overnight at 383 K and then calcined in air at 773 K for 4 h.

2.4 Preparation of dried-MMAO (dMMAO)

100 ml of MMAO solution in hexane was evacuated and washed with toluene (100 ml x 2) to remove the impurities. Then continue to wash with heptane for 6-8 times to remove TMA and TIBA in MMAO to obtain the dMMAO as white solid.

2.5 Preparation of B-modified MCM-41-supported dMMAO

The B-modified MCM-41 support was reacted with the desired amount of dMMAO in 20 ml of toluene at room temperature for 30 min. The solvent was then removed from the mixture by evacuated. This procedure is done for 1 time with 20 ml of toluene (20 ml x 1) and 3 times of hexane (20 ml x 3). Then, the solid part was dried under vacuum at room temperature. The white powder of supported cocatalyst (dMMAO/support) was then obtained.

2.6 Polymerization

The ethylene and 1-octene copolymerization reaction were carried out in a 100 ml semi-batch stainless steel autoclave reactor equipped with magnetic stirrer. In the glove box, the amount of *rac*-Et[Ind]$_2$$ZrCl_2$ and TMA were mixed and stirred for 5 min for aging. Then, toluene (to make a total volume of 30 ml) and 100 mg of dMMAO/support were introduced into the autoclave. After that, the mixture of *rac*-Et[Ind]$_2$$ZrCl_2$ and TMA were injected into the reactor. The reactor was frozen in liquid nitrogen to stop reaction

and then 0.018 mol of 1-octene was injected into the reactor. The autoclave was evacuated to remove the argon. Then, the reactor was heated up to polymerization temperature (343 K) and the polymerization was started by feeding ethylene gas (total pressure 50 psi in the reactor) until the consumption of ethylene 0.018 mol (6 psi was observed from pressure gauge). The reaction of polymerization was terminated by addition of acidic methanol. The time of reaction was recorded for purpose of calculating the activity. The precipitated polymer was washed with methanol and dried at room temperature.

2.7 Characterization

2.7.1 Characterization of support and dMMAO/support

N_2 physisorption: Measurement of BET surface area, average pore diameter and pore size distribution of MCM-41 support were determined by N_2 physisorption using a Micromeritics ASAP 2000 automated system.

X-ray diffraction: XRD was performed to determine the bulk crystalline phases of samples. It was conducted using a SIEMEN D-5000 X-ray diffractometer with CuK_α (λ = 1.54439 Å). The spectra were scanned at a rate of 2.4° min^{-1} in the range 2θ = 10-80°.

Raman spectroscopy: The Raman spectra of the samples were collected by projecting a continuous wave YAG laser of Nd (810 nm) through the samples at room temperature. A scanning range of 100-1000 cm^{-1} with a resolution of 8 cm^{-1} was applied.

X-ray photoelectron spectroscopy: XPS was used to determine the binding energies (BE) and surface concentration of samples. It was carried out using the Shimazu AMICUS with VISION 2-control software. Spectra were recorded at room temperature in high-resolution mode (0.1 eV step, 23.5 eV pass energy) for Al 2p core-level region. The samples were mounted on an adhesive carbon tape as pellets. The energy reference for Ag metal (368.0 eV for $3d_{5/2}$) was used for this study.

Thermal Gravity Analysis: TGA was performed using TA Instruments SDT Q 600 analyzer. The samples of 10-20 mg and a temperature ramping from 303 to 873 K at 5 K/min were used in the operation. The carrier gas was N_2 UHP.

2.7.2 Characterization of polymer

Gel permeation chromatography: The molecular weight and molecular weight distribution of polymer was determined using gel permeation chromatography (GPC, PL-GPC-220). Samples were prepared having approximately concentration of 1 to 2 mg/ml in trichlorobenzene (mobile phase) by using the sample preparation unit (PL-SP 260) with filtration system at a temperature of 423 K. The dissolved and filtered samples were transferred into the GPC instrument at 423 K. The calibration was conducted using the universal calibration curve based on narrow polystyrene standards.

3. Results and discussion

In this study, the catalytic activity during ethylene/1-octene copolymerization of B-modified MCM-41-supported dMMAO with a zirconocene catalyst was investigated. In fact, the MCM-41 support was prepared, then sequentially modified with B having approximately 1 and 5 wt% of B in the support, named as 1B-MCM-41 and 5B-MCM41, respectively. The B-modified MCM-41 supports were then characterized using XRD and Raman spectroscopy. The XRD patterns of the unmodified MCM-41 and B-modified MCM-41 supports are shown in **Figure 1**. It can be seen that the unmodified MCM-41 support exhibited the characteristic board peaks of the amorphous silica at ca. 10^{o} to 30^{o}. After modification with 1 wt% of B, the support still exhibited the similar XRD patterns as seen for the unmodified one. It indicated that B_2O_3 was in the highly dispersed form, which was invisible by XRD. However, when increased the B loading to 5 wt%, the XRD peaks of B_2O_3 can be detected at ca. 14.6^{o} (weak) and 27.9^{o} (strong). Raman spectra of supports with and without B modification are shown in **Figure 2**. No significant Raman bands were observed for the unmodified MCM-41 support between 200 to 1000 cm^{-1}. However, the strong Raman band for B_2O_3 was observed at ca. 880 cm^{-1} for 5B-MCM-41. For the low (1 wt%) B loading sample, the characteristic Raman band at 880 cm^{-1} was only slightly observed. It should be noted that Raman spectroscopy is more of surface technique. Therefore, the observation of B with low loading at surface could be possible which was not the case for the bulk as seen by XRD.

After the impregnation of dMMAO onto the unmodified and B-modified MCM-41 supports, the ethylene/1-octene copolymerization with *rac*-Et[Ind]$_2$ZrCl_2 catalyst was

performed in the presence of supports at the same condition for a comparative study regards to the catalytic activities derived from different supports. In fact, the activation of a zirconocene catalyst with methylaluminoxane compound has been reported elsewhere.[21] The activities of catalyst via various supports are listed in **Table 1**. It was obvious that the homogeneous catalytic system provided the highest activity among the supported catalytic system due to the absence of support interaction. Considering the supported system, it can be observed that the B-modified MCM-41 exhibited higher activity than the unmodified MCM-41 almost 2 times for both the 1B-MCM-41 and 5B-MCM41 supports. It should be noted that an increase in the amount of B loading apparently resulted in a slight decrease in the catalytic activity. In order to determine the effect of B modification, XPS measurement on the various supports was conducted. The binding energy (BE) for B 1s and Al 2p along with the surface concentrations of $[B]_{Support}$ and $[Al]_{dMMAO}$ were measured. The XPS profiles (not shown) for the typical B 1s (BE ~ 192.5-192.8 eV) and Al 2p (BE ~ 74.6-74.8 eV) on various supports in this study were similar. It should be mentioned that the BE of Al 2p was also in accordance with those on silica reported by Shiono group.[22] This was suggested that no significant change in the oxidation state of B (support) and Al (dMMAO) upon the various supports employed. The surface concentrations of $[B]_{Support}$ and $[Al]_{dMMAO}$ measured by XPS are shown in **Table 2**. Considering the surface concentrations of B in different modified supports, it was found that for 1B-MCM-41, B (~ 1.2 wt% at surface) was mostly located on the surface of MCM-41 whereas most of B was in the bulk for the 5B-MCM-41 indicating that only one forth of B (only 1.3 wt% at surface) was located at surface. The surface concentrations of Al as shown in **Table 2** were also varied upon the different supports employed. It can be observed that the surface concentrations for the unmodified and 1B-MCM-41 supports were similar (~26.5-26.8 wt%). Although they had the equal amount of Al concentration at surface, the 1B-MCM-41 exhibited dramatically higher activity than the unmodified MCM-41 support almost 2 times. This indicated that B modification would result in a decreased interaction between the support and dMMAO. As a result, activity pronouncedly increased with B modification. However, with increased B loading in the support (5B-MCM-41), the surface concentration of Al apparently decreased significantly. This was presumably due to the migration of Al into the B layer. The lesser amount of surface concentrations of Al would be the main reason for the decreased activity observed in the 5B-MCM-41 support compared to the 1B-MCM-41 support. It was worth noting that even though the surface concentration of $[Al]_{dMMAO}$ for the

unmodified MCM-41 support was essentially higher than that of the 5B-MCM-41, the unmodified MCM-41 support exhibited such a lower activity. This was suggested that the stronger support interaction in the unmodified MCM-41 support played more important role on the decreased activity than the amount of dMMAO at surface did. Hence, the unmodified MCM-41 gave lower activity than the 5B-MCM-41 (lesser amount of $[Al]_{dMMAO}$ at surface) did. On the other hand, strong support interaction was the key factor (not the surface concentrations of $[Al]_{dMMAO}$) to determine the catalytic activity for this catalytic system. It can be proposed that B can act as a spacer to anchor the support and dMMAO leading to fewer interactions. In order to give a better understanding for the effect of B modification on surface concentrations and strong support interaction as mentioned earlier, the suggested model is also illustrated as shown in **Scheme 1**.

The TGA measurement was performed to proof the interaction between the $[Al]_{dMMAO}$ and various supports. The TGA profiles of $[Al]_{dMMAO}$ on various supports are shown in **Figure 3** indicating the similar profiles for various supports. It was observed that the weight loss of $[Al]_{dMMAO}$ present on various supports were in the order of 5B-MCM-41 (20%) > 1B-MCM-41 (17%) > MCM-41 (13%). The species having strong interaction with the support was removed at ca. 553, 563 and 606 K for 5B-MCM-41, 1B-MCM-41 and MCM-41, respectively. This indicated that $[Al]_{dMMAO}$ present on MCM-41 without B modification had the strongest interaction, thus, lowest polymerization activity was observed.

Besides the effect of B modification on the catalytic activity, it would be very interesting to further investigate how this affected the polymer properties in terms of molecular weights (MW) and molecular weight distribution (MWD). As known, the MW and MWD are two of the most important properties used to classify the application of polymer. The MW and MWD of polymer obtained from different supports are shown in **Table 3**. Based on the GPC curve (not shown), only the unimodal molecular weight distribution of polymer was obtained. It can be observed that B modification apparently resulted in a slight increase in MW of polymer produced. This was suggested that inhibition of chain transfer reaction during polymerization could be achieved with the B modification on MCM-41 support. Furthermore, it was worth noting that the narrower

MWD was also evident for B modification indicating more uniform catalytic sites occurred.

4. Conclusions

Based on the present study, it can be concluded that the enhanced catalytic activity can be achieved via B-modified MCM-41 support for the supported dMMAO/zirconocene catalyst during ethylene/1-octene copolymerization. Boron can act as a spacer to anchor the support and dMMAO leading to a decreased interaction. However, larger amounts of B loading turned to a slight decrease in activity due to the migration of Al (dMMAO) into B layer. In addition, the MW of polymer was found to slightly increase with the B modification due to inhibition of chain transfer reaction during polymerization. Besides, the narrower MWD of polymer was also obtained with B modification on the support indicating more single site nature of the catalytic system.

Acknowledgements

We thank the Thailand Research Fund (TRF), and the financial support from the graduate school at Chulalongkorn University. Guidance of the MCM-41 preparation by Dr. Panpranot is greatly appreciated.

Literature Cited

(1) Kaminsky, W.; Laban,A. Metallocene catalysis. *Appl. Catal. A.* **2001**, *222*, 47.

(2) Galland, G.B.; Seferin, M.; Mauler, R.S.; Dos Santos, J.H.Z. Linear low-density polyethylene synthesis promoted by homogeneous and supported catalysts. *Polym. Int.* **1999**, *48*, 660.

(3) Rahiala, H.; Beurroies, I.; Eklund, T.; Hakala, K.; Gougeon, R.; Trens, P.; Rosenholm, J.B. Preparation and Characterization of MCM-41 Supported Metallocene Catalysts for Olefin Polymerization. *J. Catal.* **1999**, *188*, 14.

(4) Lee, K-S.; Oh, C-G.; Yim, J-H.; Ihm, S-K. Characteristics of zirconocene catalysts supported on Al-MCM-41 for ethylene polymerization. *J. Mol. Catal. A.: Chem.* **2000**, *159*, 301.

(5) Galland, G.B.; Seferin, M.; Guimarães, R.; Rohrmann, J.A.; Stedile, F.C.; Dos Santos, J.H.Z. Evaluation of silica-supported zirconocenes in ethylene/1-hexene copolymerization. *J. Mol. Catal. A.: Chem.* **2002**, *189*, 233.

(6) Quijada, R.; Retuert, J.; Guevara, J.L.; Rojas, R.; Valle, M.; Saavedra, P.; Palza, H.; Galland, G.B. Results Coming from Homogeneous and Supprted Metallocene Catalysts in the Homo- and Copolymerization of Olefins. *Macromol. Symp.* **2002**, *189*, 111.

(7) Jongsomjit, B.; Kaewkrajang, P.; Wanke, S.E.; Praserthdam, P. A comparative study of ethylene/α-olefin copolymerization with silane-modified silica-supported MAO using zirconocene catalysts. *Catal. Lett* . **2004**, *94*, 205.

(8) Jongsomjit, B.; Praserthdam, P.; Kaewkrajang, P. A comparative study on supporting effect during copolymerization of ethylene-1-olefin with silica-supported zirconocene/MAO catalyst. *Mater. Chem. Phys.* **2004**, *86*, 243.

(9) Jongsomjit, B.; Kaewkrajang, P.; Shiono, T.; Praserthdam, P. Supporting Effects of Silica-Supported Methylaluminoxane (MAO) with Zirconocene Catalyst on Ethylene/1-Olefin Copolymerization Behaviors for Linear Low-Density Polyethylene (LLDPE) Production. *Ind. Eng. Chem. Res.* **2004**, *43*, 7959.

(10) Britcher, L.; Rahiala, H.; Hakala, K.; Mikkola, P.; Rosenholm, J.B. Preparation, Characterization, and Activity of Silica Supported Metallocene Catalysts. *Chem. Mater.* **2004**, *16*, 5713.

(11) Jongsomjit, B.; Ngamposri, S.; Preserthdam, P. Role of titania in TiO_2-SiO_2 mixed oxides-supported metallocene catalyst during ethylene/1-octene copolymerization. *Catal. Lett.* **2005**, *100*, 139.

(12) Jongsomjit, B.; Ngamposri, S.; Preserthdam, P. Catalytic Activity During Copolymerization of Ethylene and 1-Hexene via Mixed TiO_2-SiO_2-Supported MAO with *rac*-Et[Ind]$_2$$ZrCl_2$ Metallocene Catalyst. *Molecules.* **2005**, *10*, 603.

(13) Ko, Y.S.; Woo, S.I. Copolymerization of Ethylene and α-Olefin Using Et[Ind]$_2$$ZrCl_2$ Entrapped inside the regular and Small Pores of MCM-41. *Macromol. Chem. Phys.* **2001**, *202*, 739.

(14) Wang, X.D.L.; Wang, W.; Yu, H.; Wang, J.; Chen, T.; Zhao, Z.; Preparation of nano-polyethylene fibers and floccules using MCM-41-supported metallocene catalytic system under atmospheric pressure. *Eur. Polm. J.* **2005**, *41*, 797.

(15) Beck, J.S.; Vartuli, J.C.; Roth, W.J.; Leonowicz, M.E.; Kresge, C.T.; Schmitt, K.D.; Chu, C.T-W.; Olson, D.H.; Sheppard, E.W.; McCullen, S.B.; Higgins, J.B.; Schlenker, J.L. A New Family of Mesoporous Molecular Sieves Prepared with Liquid Crystal Templates. *J. Am. Chem. Soc.* **1992,** *114*, 10834.

(16) Oberhagemann, U.; Jeschke, M.; Papp, H. Synthesis of highly ordered boron-containing B-MCM-41 and pure silica MCM-41. *Micropor. Mesopor. Mater.* **1999,** *33*, 165.

(17) Sayari, A.; Danumah, C.; Moudrakovski, I.L. Boron-Modified MCM-41 Mesoporous Molecular Sieves. *Chem. Mater.* **1995,** *7*, 813.

(18) Trong On, D.; Joshi, P.N.; Kaliaguine, S. Synthesis, Stability and State of Boron in Boron-Substituted MCM-41 Mesoporous Molecular Sieves. J. *Phys. Chem.* **1996,** *100*, 6743.

(19) Charoenchaidet, S.; Chavadej, S.; Gulari, E. Borane-functionalized silica supports In situ activated heterogeneous zirconocene catalysts for MAO-free ethylene polymerization. *J. Mol. Catal. A.: Chem.* **2002,** *185*, 167.

(20) Panpranot, J.; Pattamakomsan, K.; Goodwin Jr., J.G.; Praserthdam, P. A comparative study of Pd/SiO_2 and Pd/MCM-41 catalysts in liquid-phase hydrogenation. *Catal. Commun.* **2004**, *5*, 583.

(21) Jongsomjit, B.; Ngamposri, S.; Praserthdam, P. Application of Silica/Titania Mixed Oxide-Supported Zirconocene Catalysts for Synthesis of Linear Low-Density Polyethylene. *Ind. Eng. Chem. Res.* **2005**, *44*, 9059.

(22) Hagimoto, H.; Shiono, T.; Ikeda, T. Supporting Effects of Methylaluminoxane on Living Polymerization of Propylene with a Chelating (Diamide)dimethyl titanium Complex. *Macromol. Chem. Phys.* **2004**, *205*, 19.

Table 1

Catalytic activities of the B-modified MCM-41-supported dMMAO with zirconocene catalyst during ethylene/1-octene copolymerization

System	wt% of B in support	Polymer Yield[a] (g)	Catalytic Activity[b] ($x10^{-4}$ kg Pol. $mol.Zr^{-1}.h^{-1}$)
Homogeneous	0	1.68	4.9
MCM-41	0	1.43	2.2
1B-MCM-41	1	1.47	3.8
5B-MCM-41	5	1.35	3.6

[a] The polymer yield was fixed [limited by ethylene fed and 1-octene used (0.018 mole equally)].

[b] Activities were measured at polymerization temperature of 343 K, [Ethylene]=0.018 mole, $[Al]_{dMMAO}/[Zr]_{cat}$ = 1135, $[Al]_{TMA}/[Zr]_{cat}$ = 2500, in toluene with total volume = 30 ml, and $[Zr]_{cat} = 5x10^{-5}$ M.

Table 2

XPS results for different supports

Support	BE for B 1s (eV)	BE for Al 2p[a] (eV)	Mass Concentration (%)	
			B	Al
dMMAO/MCM-41	-	74.7	-	26.5
dMMAO/1B-MCM-41	192.5	74.8	1.2	26.8
dMMAO/5B-MCM-41	192.8	74.8	1.3	19.4

[a] Al 2p from dMMAO

Table 3

Molar weight (MW) and molecular weight distribution (MWD) of polymers obtained via boron-modified MCM-41-supported-MMAO with zirconocene catalyst

System	MW[a] (x 10^{-4} g mol^{-1})	M_n[a] (x 10^{-4} g mol^{-1})	MWD[a]
Homogeneous	2.13	0.63	3.4
MCM-41	2.15	0.63	3.4
1B-MCM-41	2.61	1.02	2.6
5B-MCM-41	2.42	1.45	1.7

[a] Obtained from GPC and MWD was calculated from MW/M_n

List of Figures

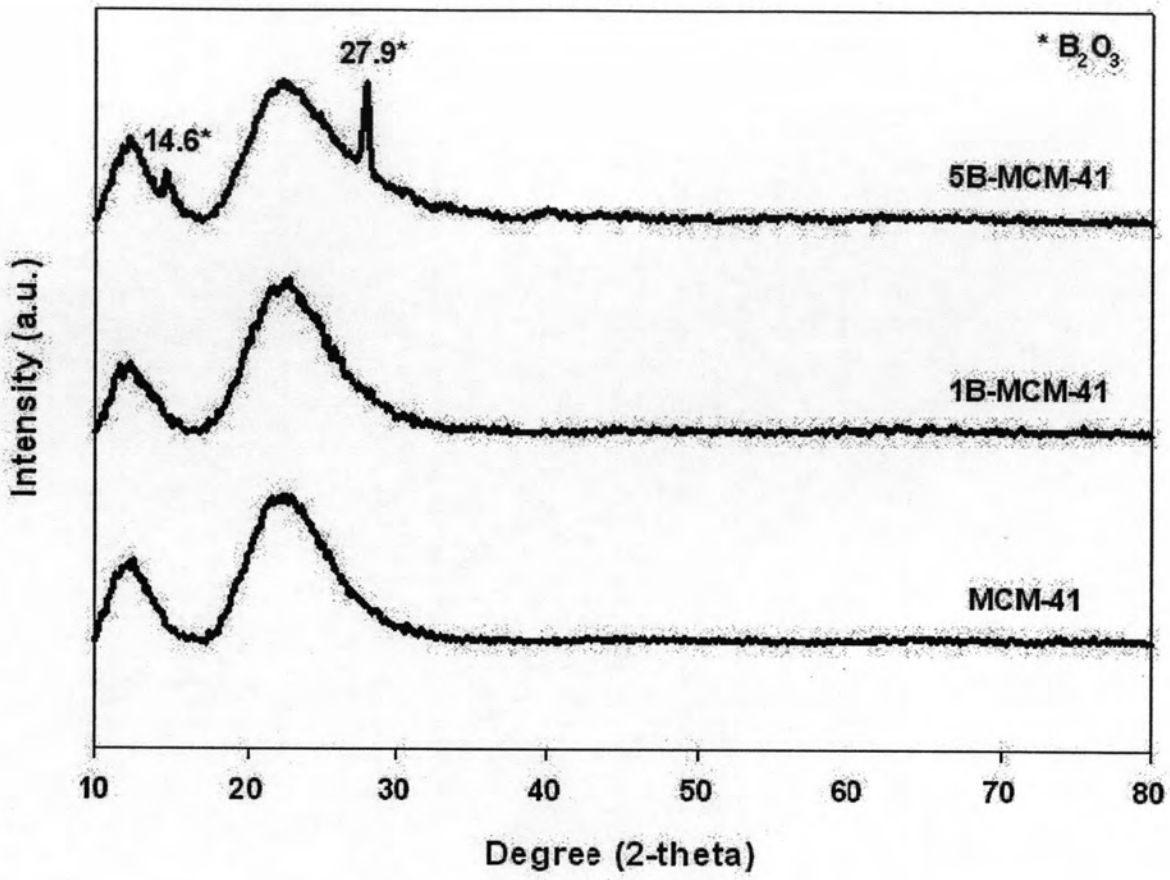
27.9*
* B_2O_3
14.6*
5B-MCM-41
1B-MCM-41
MCM-41
Intensity (a.u.)
10
20
30
40
50
60
70
80
Degree (2-theta)

Figure 1

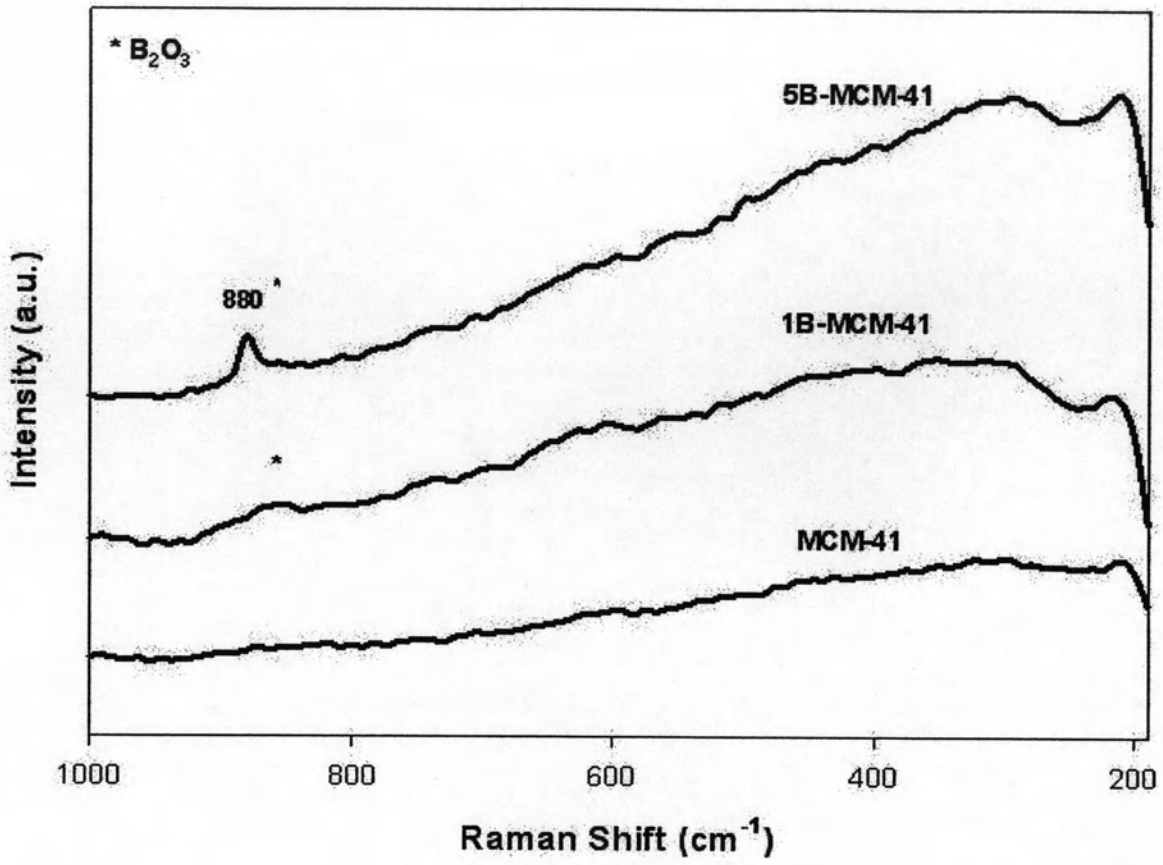
* B_2O_3
5B-MCM-41
880 *
1B-MCM-41
*
MCM-41
Intensity (a.u.)
1000
800
600
400
200
Raman Shift (cm^{-1})

Figure 2

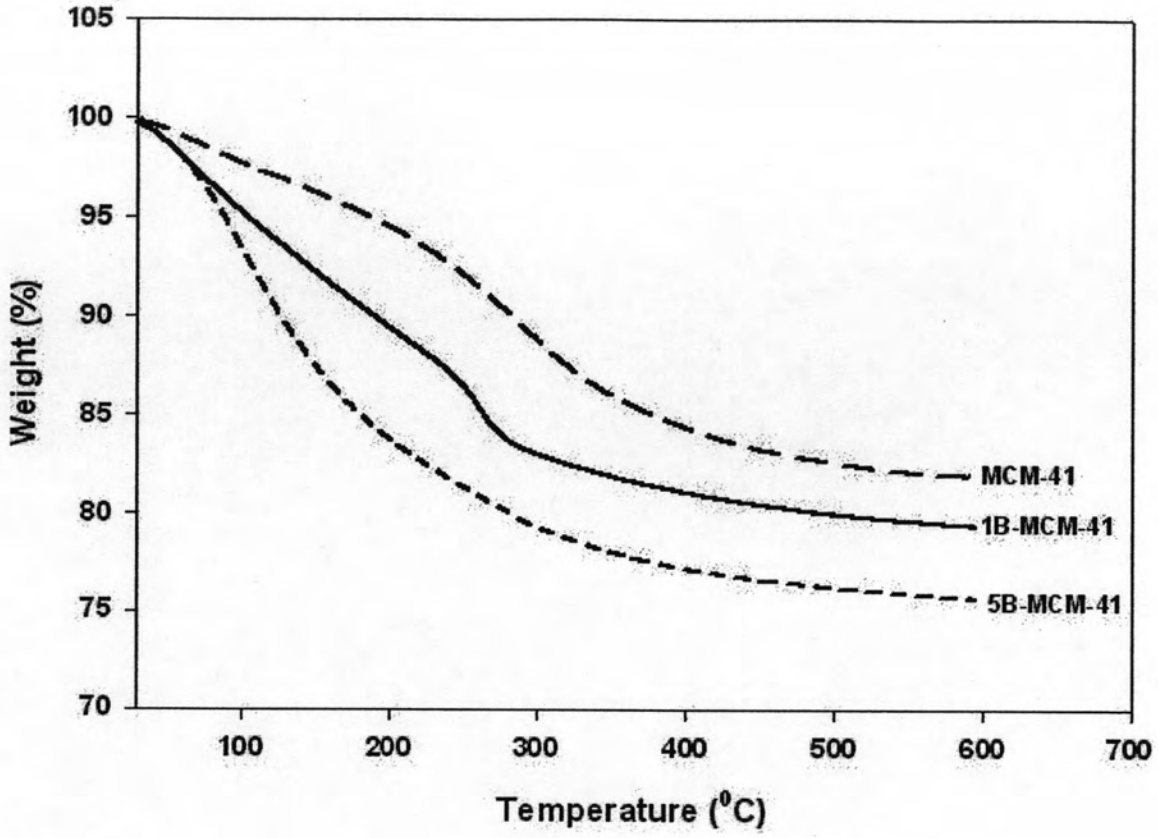
105
100
95
90
85
80
75
70
Weight (%)
100
200
300
400
500
600
700
Temperature (⁰C)
MCM-41
1B-MCM-41
5B-MCM-41

Figure 3

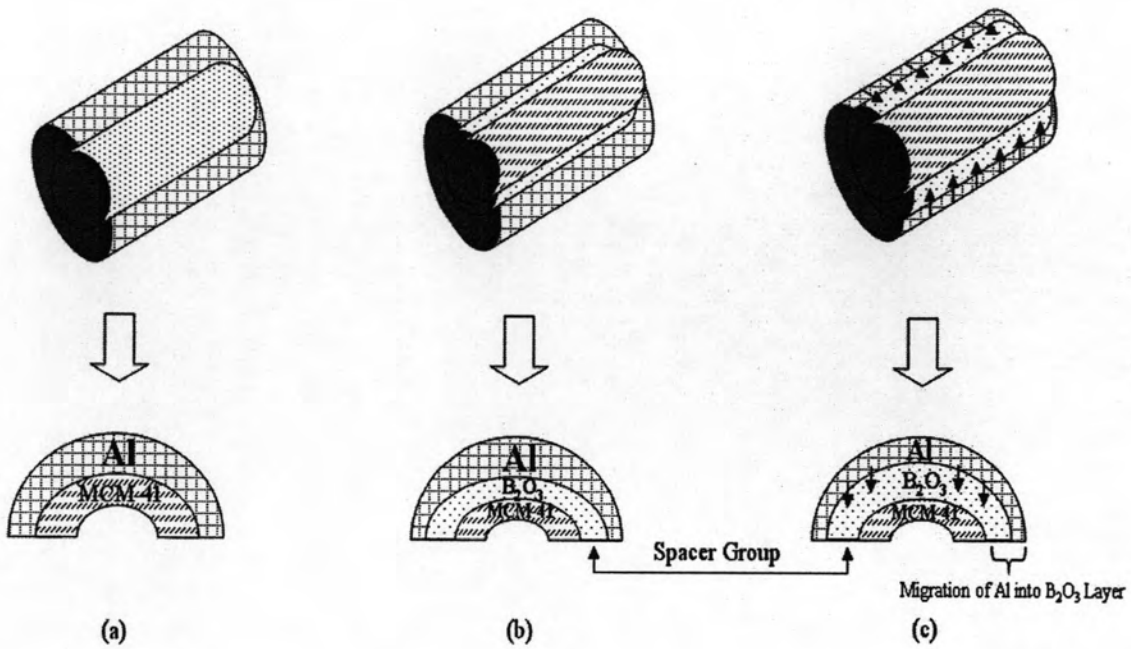
Al
MCM-41
Al
B_2O_3
MCM-41
Al
B_2O_3
MCM-41
Spacer Group
Migration of Al into B_2O_3 Layer
(a)
(b)
(c)

Scheme 1

APPENDIX H
(The Proceeding of 13th Regional Symposium on Chemical Engineering, RSCE 2006)

Copolymerization behaviors of ethylene/1-octene via boron-modified MCM41-supported zirconocene catalyst

Supaluk Jiamwijitkul, Bunjerd Jongsomjit*, and Piyasan Praserthdam

Center of Excellence on Catalysis and Catalytic Reaction Engineering
Department of Chemical Engineering, Faculty of Engineering
Chulalongkorn University, Bangkok 10330 Thailand

*Corresponding author, E-mail: bunjerd.j@chula.ac.th

ABSTRACT

Activities of ethylene/1-octene copolymerization were found to increase with boron-modified MCM-41-supported MMAO using zirconocene catalyst. Based on the XPS measurement, it revealed that the amounts of MMAO (Al 2p) at surface of MCM-41 were similar for the both boron-modified and unmodified MCM-41. Thus, increased activity with boron modification was perhaps due to decreased interaction between the MMAO and support.

1.INTRODUCTION

Since their discovery in 1992 [1], MCM-41 and related mesoporous molecular sieves attracted much attention. MCM-41 possesses unidirectional, channel-like pores of rather uniform size which are arrange in a regular hexagonal pattern. The pore diameter are adjustable in the range 15 to 100 Å depending on the synthesis conditions [2]. Many researchers investigated MCM-41 materials in which a catalytically active component was introduced. Several elements, such as Al[5 ,6] and B [2-4, 7] have been incorporated into the framework in order to generate potential catalytic activity. Therefore, a modification of the support properties is required in order to maintain high activity as in the homogeneous system or even closer.

In this present study, the ethylene/1-octene copolymerization using boron-modified MCM-41-supported with a zirconocene catalyst was investigated. The contents of boron loading used were varied. The supported catalytic systems were prepared, characterized, and tested for ethylene/1-octene copolymerization. The copolymers produced were also further characterized.

2.EXPERIMENTAL

The ethylene and 1-octene copolymerization reaction was carried out in a 100 ml semi-batch stainless steel autoclave reactor equipped with magnetic stirrer. In the glove box, the amount of $Et(Ind)_2ZrCl_2$ and TMA were mixed and stirred for 5 min. Then toluene (to make a total volume of 30 ml) and 100 mg of catalyst precursor were introduced into the autoclave. After that, the mixture of $Et(Ind)_2ZrCl_2$ and TMA were injected into the reactor. The reactor was frozen in liquid nitrogen to stop reaction and then 0.018 mol of 1-octene was injected into the reactor. The autoclave was evacuated to remove the argon. After that, the reactor was heated up to polymerization temperature and the polymerization was started by feeding ethylene gas (total pressure 50 psi) until the consumption of ethylene 0.018 mol (6 psi was observed from pressure gauge). The reaction of polymerization was terminated by addition of acidic methanol. The time of

reaction was recorded for purposes of calculating the activity. The precipitated polymer was washed with methanol and dried in room temperature.

3.RESULTS AND DISCUSSION

The catalytic activities are listed in Table 1. It can be observed that according to the heterogeneous system, activities apparently increased with the boron(B) modification on MCM-41. However, increased B loading (from 1 to 5 wt%) resulted in slightly decreased activity. The amounts of MMAO (Al 2p) at surface were determined by means of XPS measurement. It was found that both unmodified and B-modified MCM-41 gave similar amounts of MMAO at surface (at low boron loading). Hence, it can be concluded that the interaction between MMAO and support decreased with B modification resulting in increased activity.

Table 1

Catalytic activities during ethylene/1-octene copolymerization via boron-modified MCM-41-supported-MMAO with zirconocene catalyst

System	Wt% of boron in support	Polymerization time (s)	Polymer yield [a] (g)	Catalytic activity [b] ($x10^{-4}$ kg polymer mol^{-1} Zr.h)
Homogeneous	0	82.2	1.6760	4.8934
MCM-41	0	98.4	1.4314	2.2279
1B[c]-MCM-41	1	94.8	1.4717	3.7979
5B[d]-MCM-41	5	92.4	1.3513	3.5561

[a] The polymer yield was fixed [limited by ethylene fed and 1-octene used (0.018 mole equally)].
[b] Activities were measured at polymerization temperature of 70^0 C, [Ethylene]=0.018 mole, $[Al]_{MMAO}/[Zr]$ = 1135, $[Al]_{TMA}/[Zr]$ = 2500, in toluene with total volume = 30 ml, and [Zr]= $5x10^{-5}$ M.
[c] Refers to loading of 1 wt% boron on the MCM-41-support.
[d] Refers to loading of 5 wt% boron on the MCM-41-support.

Acknowledgements

We thank the Thailand Research Fund (TRF), and the financial support from the graduate school at Chulalongkorn University (90^{th} Anniversary of Chulalongkorn University).

References

[1] **Beck, J.S.** (1992). *A New Family of Mesoporous Molecular Sieves Prepared with Liquid Crystal Templates*. J. Am. Chem. Soc. 114, 10834-10843.

[2] **Obehagemann U.** (1999). *Synthesis of highly ordered boron-containing B-MCM-41 and pure silica MCM-41*. Micropor. And Mesopor. Meter. 33, 165-172.

[3] **Oberhagemann U.** (1996). *Synthesis and properties of boron containing MCM-41*. J. **Non-Crytalline Solids** 197, 145-153.

[4] **Sayari A.** (1995). *Boron-Modified MCM-41 Mesoporous Molecular Sieves.* Chem. Mater. 7 **(5),** 813-815.

[5] **Rahiala H.** (1999). *Preparation and Characterization of MCM-41 Supported Metallcene Catalysts for Olefin Polymerization.* J.Catal. 188, 14-23.

[6] **Soo Lee K.** (2000). *Characteristics of zirconocene catalysts supported on Al-MCM-41 for ethylene polymerization.* J. Mol. Catal. A : Chem. 159, 301-308.

[7] **Trang On D.** (1996). *Synthesis, Stability and State of Boron in Boron-Substituted MCM-41 Mesoporous Molecular Sieves.* J. Phys. Chem. 100, 6743-6748.

VITA

Miss. Supaluk Jiamwijitkul was born on June 18, 1982 in Chumphon, Thailand. She received the Bachelors Degree of Engineering from the Department of Chemical, Faculty of Engineering, Prince of Songkhla University in March 2005, She continued her Masters study at Chulalongkorn University in June, 2005.